



HAL
open science

Influence of hydroxybenzoic acids on the adsorption of Eu(III) onto α,γ -Al₂O₃ particles in mildly acidic conditions: a macroscopic and spectroscopic study

Pauline Moreau, Sonia Colette-Maatouk, Pierre Gareil, Pascal E. Reiller

► To cite this version:

Pauline Moreau, Sonia Colette-Maatouk, Pierre Gareil, Pascal E. Reiller. Influence of hydroxybenzoic acids on the adsorption of Eu(III) onto α,γ -Al₂O₃ particles in mildly acidic conditions: a macroscopic and spectroscopic study. *Applied Geochemistry*, 2016, 74, pp.13-23. 10.1016/j.apgeochem.2016.08.013 . cea-01375382

HAL Id: cea-01375382

<https://cea.hal.science/cea-01375382>

Submitted on 13 Sep 2019

HAL is a multi-disciplinary open access archive for the deposit and dissemination of scientific research documents, whether they are published or not. The documents may come from teaching and research institutions in France or abroad, or from public or private research centers.

L'archive ouverte pluridisciplinaire **HAL**, est destinée au dépôt et à la diffusion de documents scientifiques de niveau recherche, publiés ou non, émanant des établissements d'enseignement et de recherche français ou étrangers, des laboratoires publics ou privés.



Distributed under a Creative Commons Attribution - NonCommercial - ShareAlike 4.0 International License

Influence of hydroxybenzoic acids on the adsorption of Eu(III) onto α,γ -Al₂O₃ particles in mildly acidic conditions: a macroscopic and spectroscopic study

Pauline MOREAU^{a,1}, Sonia COLETTE-MAATOUK^{a,2}, Pierre GAREIL^b,

Pascal E. REILLER^{a,*}

^a Den – Service d'Etudes Analytiques et de Réactivité des Surfaces (SEARS), CEA, Université Paris-Saclay, F-91191, Gif sur Yvette, France. ^b Chimie ParisTech, Laboratory of Physicochemistry of Electrolytes, Colloids, and Analytical Sciences, UMR 7195, 11 rue Pierre et Marie Curie, F-75005, Paris, France.

Keywords

Europium; alumina; phenolic acids; adsorption; TRLS

* Corresponding author: pascal.reiller(at)cea.fr

Present address

¹BRGM, Direction des Laboratoires, 3 Avenue Claude Guillemin – BP 36009, 45060 Orléans CEDEX 02, France.

²Commissariat à l'Énergie Atomique et aux Énergies Alternatives, CE Saclay, DEN/DPIE/SA2P, Bâtiment 516P, 91191 Gif-sur-Yvette CEDEX, France.

<http://dx.doi.org/10.1016/j.apgeochem.2016.08.013>

ABSTRACT

The influence of hydroxybenzoic acids (HAH_n), namely *p*-hydroxybenzoic acid (4-hydroxybenzoic acid, HPhbH) and protocatechuic acid (3,4-dihydroxybenzoic acid, HProtoH₂), on the adsorption of europium(III) onto α,γ -Al₂O₃ particles is studied as a function of acid concentration. After measuring the adsorption edge of the Eu(III)/ α,γ -Al₂O₃ binary system, and using the previously studied binary component system Eu(III)/HAH_n—Moreau et al. (2015) *Inorg. Chim. Acta* **432**, 81—, and HAH_n/ α,γ -Al₂O₃—Moreau et al. (2013) *Colloids Surf. A* **435**, 97—, it is evidenced that HPhbH does not enhance Eu(III) adsorption onto α,γ -Al₂O₃ in the Eu(III)/HPhbH/ α,γ -Al₂O₃ ternary system. Conversely, HProtoH₂ enhances Eu(III) adsorption onto α,γ -Al₂O₃ in the Eu(III)/HProtoH₂/ α,γ -Al₂O₃ ternary system. Adsorption of the acids are also found higher in the Eu(III)/acid/ α,γ -Al₂O₃ ternary systems as compared with the corresponding binary systems assessing synergetic effects. For high HPhbH concentrations, a ternary surface species involving $\equiv\text{AlOH}$ surface sites, Eu(III), and PhbH⁻ is evidenced by time-resolved luminescence spectroscopy (TRLS). However, in the Eu(III)/HProtoH₂/ α,γ -Al₂O₃ ternary system, chemical environment of Eu(III) is found to be very close to that in the Eu(III)/HProtoH₂ binary system. Ternary surface species could not be evidenced in the Eu(III)/HProtoH₂/ α,γ -Al₂O₃ ternary system with TRLS because of the very short decay time of Eu(III) in the presence of protocatechuic acid.

1. INTRODUCTION

The fate of radionuclides (RNs) in the environment, and among them americium(III) and curium(III) that are both showing high chemical and radiological toxicities, is governed by their interactions with mineral surfaces and natural organic molecules. Both of these soil components may modify speciation, bioavailability and mobility of RNs. Indeed, organic acids present in soils are involved in several geochemical processes, such as complexation

with metal-ions (Aoyagi et al., 2004; Aydin and Özer, 2004; Hasegawa et al., 1989; Jejurkar et al., 1972; Kuke et al., 2010; Marmodée et al., 2009; Moreau et al., 2015; Primus and Kumke, 2012; Wang et al., 1999) oxide dissolution (Furrer and Stumm, 1986; Johnson et al., 2005; Molis et al., 2000; Stumm, 1997; Stumm and Morgan, 1996) and *pH* buffering. They may also have an influence on the adsorption of RNs onto mineral surface.

Depending on experimental conditions—*i.e.*, *pH*, acid nature, and concentration—organic acids can form stable complexes in solution resulting in a decrease in the amount of adsorbed cation (Alliot et al., 2005b) or, on the contrary, can lead to synergistic effects resulting in increasing cation adsorption *via* mixed complex formation (Alliot et al., 2006; Alliot et al., 2005a; Alliot et al., 2005b; Bourg and Schindler, 1978; Janot et al., 2011; Lenhart et al., 2001; Schindler, 1991) or have quite no effect on adsorption of RNs (Rabung et al., 1998a).

Hydroxybenzoic acids are antioxidant and antifungi naturally present in soils, degradation products of lignin, and paraben precursors. They can be considered as the first step to describe natural organic matter (NOM) as these molecules have chemical functional groups that are found in NOM, namely carboxylic and phenolic groups. Among these molecules are *p*-hydroxybenzoic acid (4-hydroxybenzoic acid, HPhbH) and protocatechuic acid (3,4-dihydroxybenzoic acid, HProtoH₂), which interactions with Eu(III) (Moreau et al., 2015) and with α,γ -Al₂O₃ particles (Moreau et al., 2013) have already been reported. They differ from each other by adding an OH-group to the benzoic ring in the meta position with respect to the carboxylate group (Fig. 1).



Fig. 1. Structures of *p*-hydroxybenzoic acid (HPhbH, left), and protocatechuic acid (HProtoH₂, right).

Europium is a lanthanide that is part from the rare-earth elements family, whose use in modern industry (Binnemans et al., 2013) and presence in the environment (Censi et al., 2013; Moermond et al., 2001) are increasing. ¹⁵²Eu isotope is a fission product produced in nuclear reactors. In addition to its particular interest, it has been widely used in speciation studies as a chemical analogue of Am(III) and Cm(III), particularly for O-containing ligands (Pearson, 1963). Europium(III) also possesses luminescent properties that permit analyzing its chemical environment in solution in a non-invasive way using time-resolved luminescence spectroscopy (TRLS) (Claret et al., 2008; Janot et al., 2011; Marang et al., 2009; Marques Fernandes et al., 2010; Moreau et al., 2015; Rabung et al., 2000; Reiller et al., 2011; Takahashi et al., 2000; Vercouter et al., 2005).

Pure Al₂O₃ does not often occur in nature but its surface sites are showing properties similar to those of aluminol sites in non-stratified clays (Marques Fernandes et al., 2010). Its adsorption properties are compared to that of hematite and goethite (Rabung et al., 1998b). It also permits to work with TRLS avoiding luminescence quenching from the oxide, as is the case with iron oxides (Claret et al., 2005).

The aim of this study is to determine the influence of hydroxybenzoic acids on the adsorption of Eu(III) onto the surface of α,γ -Al₂O₃ in mildly acidic conditions at a relatively low ionic

strength, which corresponds to a forest soil. At the macroscopic scale we are quantifying Eu(III) and hydroxybenzoic acids adsorption onto the mineral surface, and at the microscopic scale we are studying the chemical environment of Eu(III) using TRLS. In this study a binary component system is composed of two entities among Eu(III), HAH_n —as for a preceding work (Moreau et al., 2015), HAH_n symbolism is chosen to distinguish the carboxylic proton, on the left hand side, from the phenolic ones, on the right hand side—, and $\alpha,\gamma\text{-Al}_2\text{O}_3$; a ternary system is containing the three entities altogether, *i.e.*, $\text{Eu(III)/HAH}_n/\alpha,\gamma\text{-Al}_2\text{O}_3$.

2. EXPERIMENTAL SECTION

2.1. Samples preparation.

All solutions were prepared using freshly purified water delivered by a Thermo EASYPURE II (Saint-Herblain, France). HPhbH , HProtoH_2 , and NaCl were purchased from Sigma-Aldrich (Saint-Quentin-Fallavier, France). HPhbH and HProtoH_2 are carrying carboxylic and phenolic functionalities. HProtoH_2 is known to be photooxidized in the presence of dioxygen at mildly alkaline pH (Hatzipanayioti et al., 2006). The $\log_{10}K^\circ$ values of the acid base reactions (Smith et al., 1998) and complex formation (Hummel et al., 2002; Moreau et al., 2015) are recalled in Table 1. The corresponding speciation diagrams at the ionic strength of the study (*vide infra*) are given in Fig. S1 of the Supplementary Information (SI).

Stock solutions of the hydroxybenzoic acids (10 mM for HPhbH , and 20 mM for HProtoH_2) were obtained from their dissolution in 10 mM NaCl . Europium stock solution (1 mM) was obtained from the dissolution of 99.99 % Eu_2O_3 (Johnson Matthey, Roissy, France) in 3.5 mM HCl . Dry $\alpha,\gamma\text{-Al}_2\text{O}_3$ particles (predominantly γ phase, with 5-20% α phase, pure 99.98% metal basis, mean particle size 0.26 μm , BET specific surface area 110 m^2/g) were purchased from Alfa Aesar (Schiltigheim, France). Colloid stock suspensions were prepared in a glovebox by introducing the $\alpha,\gamma\text{-Al}_2\text{O}_3$ powder in 30 mL of 10 mM NaCl , acidified with HCl

to *pH* 4.0. Then the suspensions were sonicated at amplitude 6 for 10 min with a Misonix sonicator 4000 (Misonix Sonicators, Newton, USA) equipped with a cup horn thermostated at 8°C. The suspensions were stirred for at least 7 days before use to allow equilibration of the surface (Lefèvre et al., 2002). Sonication was repeated just before preparation of binary systems. The alumina surface properties have been reported by Moreau et al. (2013).

Table 1. Values of $\log_{10}K^\circ$ for the different reactions considered. All these constants were corrected from non-ideality using Kielland (1937).

Reaction	$\log_{10}K^\circ$	
Eu(III) inorganic species		
$\text{Eu}^{3+} + \text{Cl}^- \rightleftharpoons \text{EuCl}^{2+}$	1.1	Hummel et al. (2002)
$\text{Eu}^{3+} + \text{H}_2\text{O} \rightleftharpoons \text{EuOH}^{2+} + \text{H}^+$	-7.64	Hummel et al. (2002)
$\text{EuOH}^{2+} + \text{H}_2\text{O} \rightleftharpoons \text{Eu}(\text{OH})_2^+ + \text{H}^+$	-7.46	Hummel et al. (2002)
HPhbH		
$\text{HPhbH} \rightleftharpoons \text{PhbH}^- + \text{H}^+$	-4.58	Smith et al. (1998)
$\text{PhbH}^- \rightleftharpoons \text{Phb}^{2-} + \text{H}^+$	-9.46	Smith et al. (1998)
$\text{Eu}^{3+} + \text{PhbH}^- \rightleftharpoons \text{EuPhbH}^{2+}$	2.18	Moreau et al. (2015)
HProtoH ₂		
$\text{HProtoH}_2 \rightleftharpoons \text{ProtoH}_2^- + \text{H}^+$	-4.49	Smith et al. (1998)
$\text{ProtoH}_2^- \rightleftharpoons \text{ProtoH}^{2-} + \text{H}^+$	-8.75	Smith et al. (1998)
$\text{ProtoH}^{2-} \rightleftharpoons \text{Proto}^{2-} + \text{H}^+$	-13	Smith et al. (1998)
$\text{Eu}^{3+} + \text{ProtoH}_2^- \rightleftharpoons \text{EuProtoH}_2^{2+}$	2.72	Moreau et al. (2015)

The *pH* values of all the solutions and the suspensions were adjusted to 5—in order to avoid the photooxidation of HProtoH₂ in the presence of dioxygen (Hatzipanayioti et al., 2006)—by adding drops of freshly prepared 1 M NaOH or HCl. The *pH* value was measured using a combined glass electrode (Mettler-Toledo, Viroflay, France) connected to a Seven Easy S20 Mettler-Toledo *pH*-meter. The electrode was calibrated externally using three commercial buffer solutions (*pH* 4.01, 7.01, 10.00) from Mettler-Toledo. Uncertainties of the calibrations were in the span 0.05-0.08. Binary and ternary systems were equilibrated under stirring for 3 days before direct analysis of the suspension with TRLS or electrophoretic mobility, and

finally centrifuged at 10 000 rpm for 90 min for determination of Eu(III) and acid concentration.

2.2. Preparation of Eu(III)/ α,γ -Al₂O₃ binary systems.

Stock solution of Eu(III) and stock suspension of α,γ -Al₂O₃ were used. All the samples were prepared in polypropylene vessels. Adsorption isotherm of Eu(III) onto α,γ -Al₂O₃ was determined at pH 6.0, C(α,γ -Al₂O₃) of 0.25 g L⁻¹, and [Eu(III)] was varied from 0 to 3 mM at an ionic strength (*I*) fixed at 20 mM NaCl. This low ionic strength was chosen in order to provide an ionic medium that is suitable for α,γ -Al₂O₃ colloidal suspension stability. Adsorption as a function of pH is studied from pH 4 to 8, at C(α,γ -Al₂O₃) = 0.5 g L⁻¹, [Eu(III)] = 10 μ M, and *I* = 20 mM NaCl. The changes in the luminescence of Eu(III) vs. pH (4.70, 5.25, 6.15, 6.65 and 7.05) were recorded at C(α,γ -Al₂O₃) = 0.5 g L⁻¹, [Eu(III)] = 10 μ M, and *I* = 10 mM NaCl.

2.3. Preparation of Eu(III)/HAH_n/ α,γ -Al₂O₃ ternary systems.

Stocks solutions were used to prepare samples with *I* = 10 mM NaCl, C(α,γ -Al₂O₃) = 0.5 g L⁻¹, [Eu(III)] = 10 μ M and increasing amount of HPhbH and HProtoH₂, from 0.05 mM to 4.5 mM.

2.4. Determination of the aqueous hydroxybenzoic acid concentration.

Absorbance spectra were recorded in a 1 cm quartz cuvette using a UV2550PC-CE Spectrophotometer (Shimadzu, Marne-la-Vallée, France). UV/Vis spectra were recorded at 20 °C between 200 nm and 600 nm and pH of all studied samples was set *ca.* 5 by adding drops of 1 mol L⁻¹ HCl or NaOH. Concentrations of HPhbH and HProtoH₂ were determined in the supernatants at 247 nm and 253 nm, respectively, using 7-point calibration curves in the range 8 μ M to 200 μ M. Some samples were diluted before analysis to meet the concentration range of the calibration curve.

2.5. Determination of total Eu and Al concentration.

The concentrations of total Eu and Al in supernatants were measured by inductively coupled plasma optical emission spectroscopy (ICP-OES) with an Optima 2000 DV Spectrometer (Perking Elmer). Eu concentrations were determined at wavelengths 412.970 nm and 381.967 nm using 5- or 6-point calibration curves (0 to 10 000 ppm). Concentrations of Al were determined at wavelengths 396.153 nm and 308.215 nm using a 5-point calibration curve (0 to 10 000 ppm). All uncertainties were better than 5%. Some samples were diluted before analysis to meet the concentration range of the calibration curve.

2.6. Time-Resolved Luminescence Spectroscopy (TRLS).

The excitation laser beam was generated by a 355 nm tripled output of a continuum Nd:YAG laser (Continuum, Excel Technology, Villebon-sur-Yvette, France) coupled to an optical parametric oscillator system (Panther, Continuum, Santa Clara, CA). The TRLS signal was collected at 90° and focused onto a 1 mm slit Acton spectrometer equipped with a 600 lines/mm grating (Princeton, Evry, France). The CCD chip of the camera was cooled down at -15°C. For the time-resolved spectra acquisition, the luminescence signal was collected during a time gate width (W) of 300 μ s, at an initial delay time (D) of 10 μ s after the excitation laser flash. The emission spectra were recorded at 22°C. For the decay time determination, the number times steps varied from one sample to another depending on the remaining luminescence after each delay. The acquisitions were stopped when the luminescence became inferior to the background noise. To increase the signal-to-noise ratio, 300 to 1000 accumulations were performed for each spectrum. All measurements were carried out at room temperature (20° C). The excitation wavelength was set at $\lambda_{\text{exc}} \approx 394$ nm, *i.e.* in the ${}^5\text{L}_6 \leftarrow {}^7\text{F}_0$ transition of Eu^{3+} (Carnall et al., 1968). For each obtained spectrum a background correction was performed, consisting in subtracting background noise from each spectrum. Then, the luminescence was divided by the incident laser energy during the

acquisition and by the number of acquisitions. In that manner, all the spectra are directly comparable.

After inner conversion from the 5L_6 excited state, the transitions from the 5D_0 excited state to the ground 7F_j manifold are responsible for the recorded luminescence (Bünzli, 1989). In the acquisition window, these transitions are the $^5D_0 \rightarrow ^7F_0$ transition ($\lambda_{\max} \approx 580$ nm), which is a dipolar magnetic and electric transition, that is theoretically forbidden, the $^5D_0 \rightarrow ^7F_1$ transition ($\lambda_{\max} \approx 592$ nm), which is a dipolar magnetic transition, and the $^5D_0 \rightarrow ^7F_2$ transition ($\lambda_{\max} \approx 618$ nm), which is described as a hypersensitive transition (Jørgensen and Judd, 1964) as it is highly correlated to the chemical environment of Eu(III).

The luminescence decay is described by a first order kinetics, and for a purely integrative system like a CCD camera the luminescence signal is given by equation (1):

$$F_i = \int_D^{D+W} F_i^0 \exp\left(-\frac{t}{\tau_i}\right) dt = F_i^0 \tau_i \exp\left(-\frac{D}{\tau_i}\right) \left[1 - \exp\left(-\frac{W}{\tau_i}\right)\right] \quad (1)$$

where F_i^0 and τ_i are the initial luminescence intensity and decay time of the i^{th} species, respectively.

The luminescence decays were fitted with to a non-linear procedure, and the standard deviations were evaluated using the Microsoft Excel Macro SolverAid (de Levie, 2005). The main drawback of this method is the difficulty to discriminate excited species that are showing very close τ_i values. Only both the determination of τ_i and the analysis of the spectra for various delay times would permit to evidence multi-exponential decay (Saito et al., 2010).

The peak area ratio between the $^5D_0 \rightarrow ^7F_2$ and the $^5D_0 \rightarrow ^7F_1$ transitions, referred as the asymmetry ratio $^7F_2/^7F_1$, were used to characterize chemical environment of Eu(III). For the sake of comparison, the intensities of the spectra presented in this work are normalized in

different ways: to the ${}^5\text{D}_0 \rightarrow {}^7\text{F}_1$ transition maximum (592 nm, the average value of five points around the maximum is taken); to the ${}^5\text{D}_0 \rightarrow {}^7\text{F}_1$ area; and to the total area of the spectrum between 570 nm and 640 nm.

3. RESULTS

In the following, for both binary and ternary systems, the time-resolved luminescence data will first be presented and discussed. The adsorption results will be presented afterwards. The link between spectroscopic (microscopic) data and adsorption (macroscopic) results will be made, whenever possible, and their relevance discussed.

3.1. Binary Eu(III)/ $\alpha,\gamma\text{-Al}_2\text{O}_3$ system

3.1.1. Luminescence of Eu(III) in binary Eu(III)/ $\alpha,\gamma\text{-Al}_2\text{O}_3$ for pH 4.7 to 7.05.

Luminescence spectra in Eu(III)/ $\alpha,\gamma\text{-Al}_2\text{O}_3$ binary system at pH values between 4.7 and 7.05 are shown in Fig. S2a of the SI together with a spectrum of Eu(III) at pH 4 and $I = 10$ mM NaCl. The spectra are normalized to their total area in the wavelength span 570-640 nm. The ${}^5\text{D}_0 \rightarrow {}^7\text{F}_0$ transition relative intensity increases with pH. The peak corresponding to the electric dipole ${}^5\text{D}_0 \rightarrow {}^7\text{F}_1$ transition is also broadened as pH increases indicating a strong change in the symmetry around Eu(III). Finally, the relative intensity of the magnetic dipole ${}^5\text{D}_0 \rightarrow {}^7\text{F}_2$ hypersensitive transition increases sharply, further evidencing that the chemical environment of Eu(III) is modified. For pH 6.65 and 7.05, the spectra obtained for $D = 10$ μs are mostly identical, which is an indication of the same speciation. The asymmetry ratio ${}^7\text{F}_2/{}^7\text{F}_1$, which permits to characterize Eu(III) speciation (Dobbs et al., 1989; Moreau et al., 2015; Rabung et al., 2000) are presented together in Fig. 2a with comparable results (Janot et al., 2011, 2013; Rabung et al., 2000). A value of ${}^7\text{F}_2/{}^7\text{F}_1 = 0.5$ is obtained for pH < 5, and increases at higher pH values.

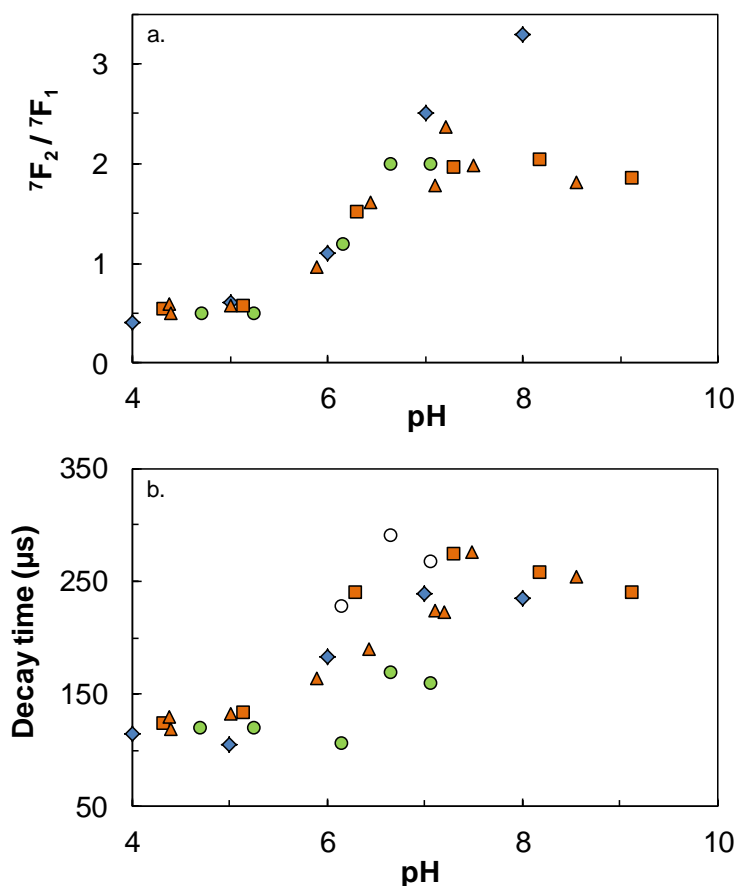


Fig. 2. Asymmetry ratio (${}^7F_2/{}^7F_1$) (a) and decay time (b) as a function of pH for Eu(III)/ α,γ -Al₂O₃ binary systems: circles, $C(\alpha,\gamma\text{-Al}_2\text{O}_3) = 0.5 \text{ g L}^{-1}$, $[\text{Eu(III)}] = 10 \text{ }\mu\text{M}$, $I = 10 \text{ mM NaCl}$, filled circles, mono-exponential (or τ_1 value), open circles τ_2 value from this work when bi-exponential decay is evidenced; diamonds, Rabung et al. (2000) $C(\alpha,\gamma\text{-Al}_2\text{O}_3) = 0.57 \text{ g L}^{-1}$, $[\text{Eu(III)}] = 3.2 \text{ }\mu\text{M}$, $I = 100 \text{ mM NaClO}_4$. Triangles and squares, Janot et al. (2011) $C(\alpha\text{-Al}_2\text{O}_3) = 1 \text{ g L}^{-1}$, $[\text{Eu(III)}] = 1 \text{ }\mu\text{M}$, $I = 100 \text{ mM}$ and 10 mM NaClO_4 , respectively.

The luminescence decay in the different Eu(III)/ α,γ -Al₂O₃ binary systems are presented in Fig. S3a to Fig. S7a of the SI, and analysed using mono-exponential and/or bi-exponential fitting. Fig. S3b to Fig. S7b of the SI are showing the residuals of these fittings; The insets to Fig. S3a to Fig. S7a of the SI are showing the spectra normalized to the 570-640 nm wavelength span, which can help evidencing differences between the spectra at different delay (D) values.

Table S1 to Table S5 of the SI are showing the correlation matrices. The obtained decay times are presented in Table S7 of the SI. Relationships between the radiative constant ($k = \tau^{-1}$) and the number of water molecules in the first hydration sphere of Eu(III) (Horrocks and Sudnick, 1979; Kimura and Choppin, 1994) allows estimating the hydration of the adsorbed species. Application of the operational relationship proposed by Kimura and Choppin (1994) to the obtained decay times are also presented in Table S7 of the SI. The decrease of the remaining number of water molecules in the first hydration sphere is also a strong indication of modification of the chemical environment of adsorbed Eu(III).

3.1.2. Adsorption of Eu(III), and influence on α,γ -Al₂O₃ dissolution

The adsorption isotherm of Eu(III) onto α,γ -Al₂O₃ at pH 6.15 is shown in Fig. S8 of the SI. The amount of adsorbed Eu(III) onto α,γ -Al₂O₃ particles increases upon increasing [Eu(III)]_{total} without reaching a plateau. It means that the adsorption of Eu(III) onto α,γ -Al₂O₃ is very high. Working with [Eu(III)] > 0.2 mM is not possible because of the possible precipitation of EuOHCO₃(s) (Hummel et al., 2002). As a comparison, the amount of occupied surface sites of α,γ -Al₂O₃ ranges from 0 to 3.5%.

The influence of HPhbH and HProtoH₂ on the dissolution of our α,γ -Al₂O₃ particles was already shown by Moreau et al. (2013). The effect of Eu(III) is also checked in Fig. S9 of the SI, where the concentration of dissolved Al vs. [Eu(III)]_{total} is given, together with the theoretical solubility of Al phases bayerite (AlOOH), α - and γ -alumina (α - and γ -Al₂O₃, respectively) at pH 5 and $I = 10$ mM NaCl—for thermodynamic data on Al, see Table 1 in Moreau et al. (2013). No particular influence of [Eu(III)]_{total} is seen up to 50 μ M, which is higher than the maximum [Eu(III)] that will be used in the following.

3.1.3. Influence of the *pH* value on the adsorption of Eu(III) onto α,γ -Al₂O₃.

The *pH*-edge for Eu(III) adsorption onto α,γ -Al₂O₃ in Fig. 3 shows a typical evolution of the adsorption of a lanthanide or rare earth onto an Al₂O₃ surface at this metal to surface site ratio (Janot et al., 2011; Kumar et al., 2012; Marmier and Fromage, 1999; Morel et al., 2012; Rabung et al., 2000; Shiao et al., 1981). Adsorption increases steadily with increasing *pH* with a *pH*-edge between *pH* 5 and *pH* 7. This behaviour is correlated to the first hydrolysis constant of Eu(III) ($\log_{10}^* \beta_1^{\circ} = -7.64$) (Hummel et al., 2002) as observed elsewhere (Bradbury and Baeyens, 2005, 2009a, b; Guo et al., 2005; Reiller et al., 2002; Tan et al., 2007) even if there can be a dependence on total metal concentration (Huittinen et al., 2009; Schindler and Stumm, 1987). Indeed, Kumar et al. (2012) showed that adsorption of Eu(III) onto silica and γ -Al₂O₃ as a function of *pH* are very similar, whereas these phases are showing very different points of zero charge—*pzc* \approx 2 and 9 for silica and γ -Al₂O₃, respectively (Kosmulski, 2009).

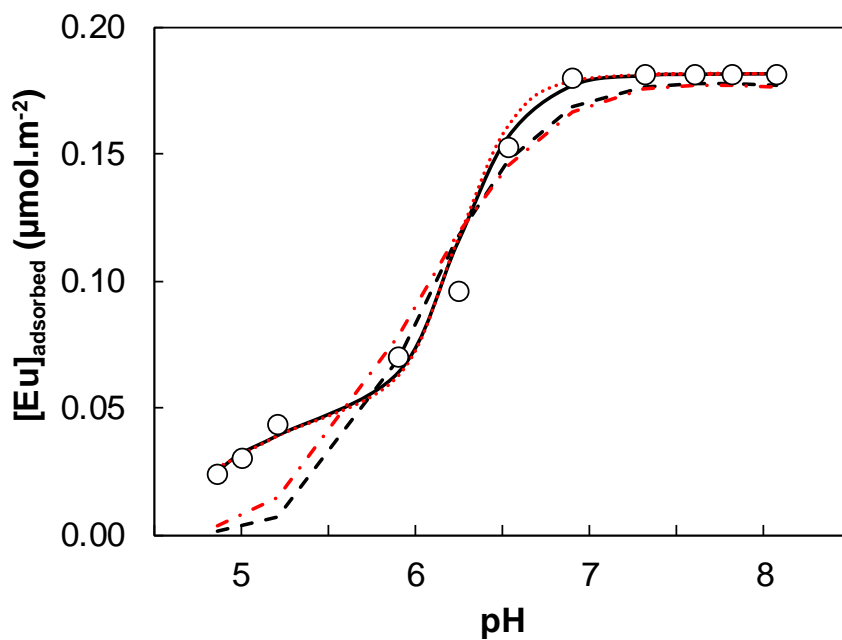


Fig. 3: The *pH*-isotherm for Eu(III) onto $\alpha,\gamma\text{-Al}_2\text{O}_3$. Experimental conditions: $C(\alpha,\gamma\text{-Al}_2\text{O}_3) = 0.5 \text{ g L}^{-1}$, $I = 20 \text{ mM NaCl}$, total initial $[\text{Eu(III)}] = 10 \text{ }\mu\text{M}$. The error bars are included into the dot thickness. Fitted curve obtained with FITEQL software (Herbelin and Westall, 1994): CCM model using 1 adsorption site, dashed line; CCM model using 2 adsorption sites, plain line; DLM model using 1 adsorption site, dash-dotted line; DLM model using 2 adsorption sites, dotted line.

Table 2: Oxide parameters by Moreau et al. (2013) and adsorption constants of Eu(III) onto α,γ -Al₂O₃ using CCM and DLM model and considering one or two adsorption sites.

		CCM*	DLM
Oxide parameters (Moreau et al., 2013)			
$\equiv\text{MOH}_2^+ \rightleftharpoons \equiv\text{MOH} + \text{H}^+$	$\log_{10}K_1$	-7.5	-8.9
$\equiv\text{MOH} \rightleftharpoons \equiv\text{MO}^- + \text{H}^+$	$\log_{10}K_2$	-9.6	-10.1
One adsorption site			
$\equiv\text{MOH} + \text{Eu}^{3+} \rightleftharpoons \equiv\text{MOEu}^{2+} + \text{H}^+$	$\log_{10}K_{\text{sorb,Eu}^{3+}}$	2.3 ± 0.2	3.4 ± 0.3
Two adsorption sites			
$\equiv\text{XOH} + \text{Eu}^{3+} \rightleftharpoons \equiv\text{XOEu}^{2+} + \text{H}^+$	$\log_{10}K_{\text{X,Eu}^{3+}}$	6.0 ± 0.9	8.4 ± 0.9
$\equiv\text{YOH} + \text{Eu}^{3+} \rightleftharpoons \equiv\text{YOEu}^{2+} + \text{H}^+$	$\log_{10}K_{\text{Y,Eu}^{3+}}$	1.2 ± 0.2	3.2 ± 0.4

* $C = 1.55 \text{ F m}^{-2}$, $N_s = 1.24 \text{ sites nm}^{-2}$ (Moreau et al., 2013)

3.2. Ternary Eu(III)/HPhbH/ α,γ -Al₂O₃ system

3.2.1. Spectroscopic results for Eu(III)

Fig. 4 presents luminescence spectra for Eu³⁺ and for the Eu(III)/HPhbH/ α,γ -Al₂O₃ ternary system— $p\text{H} = 5$, $[\text{HPhbH}]_{\text{total}} = 0.6 \text{ mM}$, $I = 10 \text{ mM NaCl}$ —normalized to the ${}^5\text{D}_0 \rightarrow {}^7\text{F}_1$ transition. The ${}^5\text{D}_0 \rightarrow {}^7\text{F}_0$ transition is visible in the ternary system, the ${}^5\text{D}_0 \rightarrow {}^7\text{F}_1$ transition does not seem to undertake modifications, and the intensity of the ${}^5\text{D}_0 \rightarrow {}^7\text{F}_2$ hypersensitive transition is almost three times higher in the ternary system as compared to free Eu³⁺.

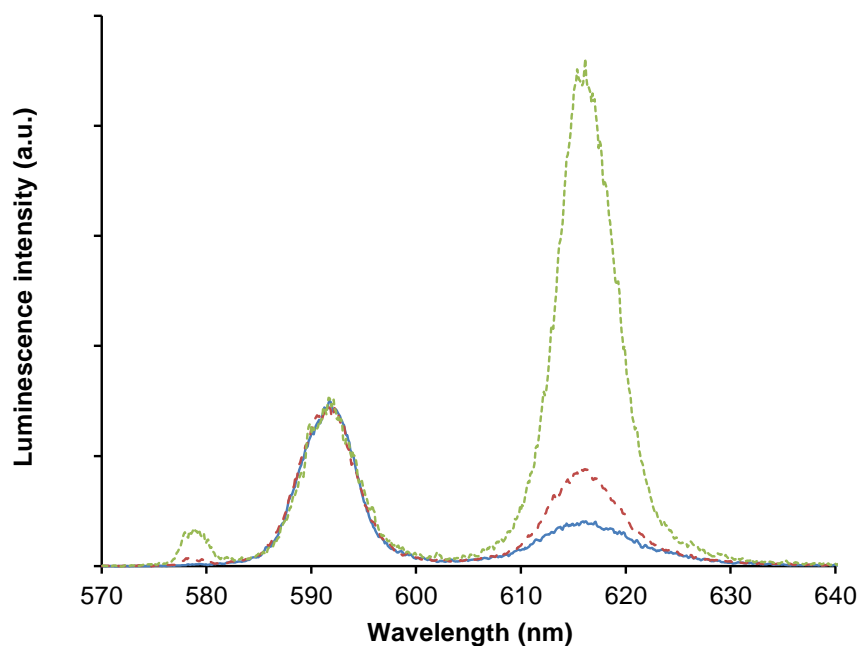


Fig. 4. Normalized TRLS spectra to the $^5D_0 \rightarrow ^7F_1$ transition of free Eu(III) (plain blue line), Eu(III)/Phb binary system (dotted green line from Moreau et al., 2015), and Eu(III)/Phb/ α,γ -Al₂O₃ ternary system (dashed red line). $C(\alpha,\gamma\text{-Al}_2\text{O}_3) = 0.5 \text{ g L}^{-1}$, $[\text{Eu(III)}] = 10 \text{ }\mu\text{M}$, $[\text{HPhbH}]_{\text{total}} = 0.6 \text{ mM}$, $p\text{H } 5$, $I = 10 \text{ mM NaCl}$.

The Eu(III)/HPhbH/ α,γ -Al₂O₃ ternary system is studied vs. $[\text{HPhbH}]_{\text{total}}$. The evolution of the asymmetry ratio and of decay times of Eu(III) luminescence are shown in Fig. 5 vs. $[\text{PhbH}^-]_{\text{total}}$, together with data from corresponding binary systems—Eu(III)/HPhbH from Moreau et al. (2015) and Eu(III)/ α,γ -Al₂O₃—, and free Eu³⁺.

It is worthwhile noting that in this ternary system decay times are mono-exponential. For $[\text{HPhbH}]_{\text{total}}$ below 0.5 mM, no difference between the binary systems and the ternary system can be evidenced. Indeed, the asymmetry ratio $^7F_2/^7F_1$ is 0.5 for all samples studied, and the decay time is approximately 110 μs . In this concentration range, adsorption of Eu(III) and HPhbH is very similar to what is obtained in binary systems. It means that the Eu(III)/HPhbH/ α,γ -Al₂O₃ ternary system can be described as the sum of binary systems when $[\text{HPhbH}]_{\text{total}} < 0.5 \text{ mM}$. The EuPhbH²⁺ complex is formed in solution and HPhbH and Eu(III)

are adsorbed onto $\alpha,\gamma\text{-Al}_2\text{O}_3$, as is the case in the binary systems $\text{HPhbH}/\alpha,\gamma\text{-Al}_2\text{O}_3$ and $\text{Eu(III)}/\alpha,\gamma\text{-Al}_2\text{O}_3$, respectively. However, differences are observed for $[\text{HPhbH}]_{\text{total}} > 0.5 \text{ mM}$ in Fig. 5a, as the asymmetry ratio in the $\text{Eu(III)}/\text{HPhbH}/\alpha,\gamma\text{-Al}_2\text{O}_3$ ternary system increases sharply compared to the $\text{Eu(III)}/\text{HPhbH}$ binary system.

Similarly, decay times in the $\text{Eu(III)}/\text{HPhbH}/\alpha,\gamma\text{-Al}_2\text{O}_3$ ternary system are higher than in the binary systems as it reaches *approx.* $130 \mu\text{s}$ (Fig. 5b). These spectroscopic differences between binary and ternary systems for $[\text{HPhbH}]_{\text{total}} > 0.5 \text{ mM}$ indicate the presence of a new species in the ternary system, involving the three partners: Eu(III) , HPhbH —probably under the form of PhbH^- —, and $\alpha,\gamma\text{-Al}_2\text{O}_3$ surface sites.

In order to study this new species in more detail, the luminescence is recorded at a delay time $D = 470 \mu\text{s}$, where the luminescence due to free Eu^{3+} — $\tau = 110 \mu\text{s} \pm 5 \mu\text{s}$ (Horrocks and Sudnick, 1979; Moreau et al., 2015)—, binary $\text{Eu(III)}/\alpha,\gamma\text{-Al}_2\text{O}_3$ — $\tau \approx 110 \mu\text{s} \pm 5 \mu\text{s}$ —, and binary $\text{Eu(III)}/\text{HPhbH}$ — $\tau \approx 107 \mu\text{s} \pm 5 \mu\text{s}$ (Moreau et al., 2015)—are negligible. As presented in Fig. S10 of the SI, for free Eu(III) and in all binary systems—even for $\text{Eu(III)}/\text{HPhbH}$ system with high $[\text{HPhbH}]_{\text{total}}$ —, luminescence of the ${}^5\text{D}_0 \rightarrow {}^7\text{F}_2$ transition is very weak and the signal is hardly over the background.

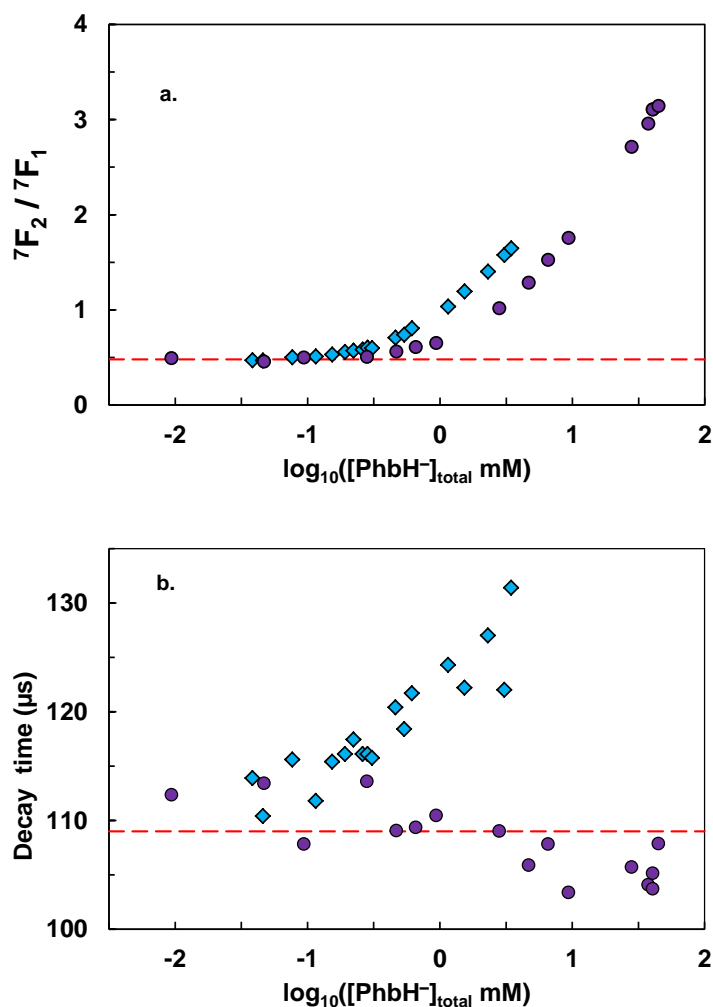


Fig. 5. Asymmetry ratio (${}^7F_2/{}^7F_1$) (a) and mono-exponential decay times (b) of Eu(III) (dashed line: data for Eu(III)/ α,γ -Al $_2$ O $_3$), Eu(III)/HPhbH (circles) from Moreau et al. (2015), and Eu(III)/HPhbH/ α,γ -Al $_2$ O $_3$ (diamonds): $C(\alpha,\gamma$ -Al $_2$ O $_3$) = 0.5 g L $^{-1}$, [Eu(III)] = 10 μ M, I = 10 mM NaCl: pH 5 for Eu(III), Eu(III)/ α,γ -Al $_2$ O $_3$, and Eu(III)/HPhbH/ α,γ -Al $_2$ O $_3$, pH 5.5 for Eu(III)/HPhbH from Moreau et al. (2015).

For ternary systems containing high total HPhbH concentration the intensity of the ${}^5D_0 \rightarrow {}^7F_2$ transition increases with $[HPhbH]_{total}$ (Fig. 6, and Fig. S10 of the SI). This evidences the presence of species other than Eu $^{3+}$ that is (are) not present in the binary systems. The decay time of the(se) species is (are) higher than 110 μ s because luminescence remains significant for a delay times of 470 μ s. A more precise determination of decay time(s) and of the number

of species is not possible because the signal becomes too low after 500 μs . Eventually, these results assess the formation of a ternary surface complex involving Eu(III), HPhbH and the $\alpha,\gamma\text{-Al}_2\text{O}_3$ surface sites with decay time close to, but slightly higher than, 110 μs .

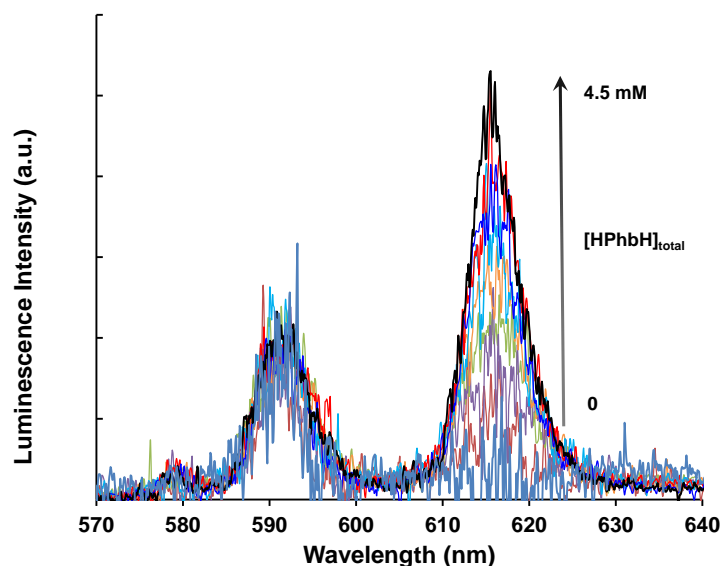


Fig. 6. TRL spectra normalized to the ${}^5\text{D}_0 \rightarrow {}^7\text{F}_1$ transition in the Eu(III)/HPhbH/ $\alpha,\gamma\text{-Al}_2\text{O}_3$ ternary system with increasing $[\text{HPhbH}]_{\text{total}}$. $C(\alpha,\gamma\text{-Al}_2\text{O}_3) = 0.5 \text{ g L}^{-1}$, $[\text{Eu(III)}] = 10 \text{ }\mu\text{M}$, $p\text{H } 5$, $I = 10 \text{ mM NaCl}$, $D = 470 \text{ }\mu\text{s}$, $W = 300 \text{ }\mu\text{s}$, $\lambda_{\text{exc}} = 394 \text{ nm}$.

3.2.2. Adsorption of HPhbH in the binary and ternary systems

The adsorption isotherms of HPhbH onto $\alpha,\gamma\text{-Al}_2\text{O}_3$ at $p\text{H } 5$ in the HPhbH/ $\alpha,\gamma\text{-Al}_2\text{O}_3$ binary system from Moreau et al. (2013) and Eu(III)/HPhbH/ $\alpha,\gamma\text{-Al}_2\text{O}_3$ ternary systems are shown in Fig. 7. HPhbH adsorption is higher in the ternary system compared to the HPhbH/ $\alpha,\gamma\text{-Al}_2\text{O}_3$ binary system, especially for $[\text{HPhbH}]_{\text{eq}} > 1 \text{ mM}$. It means that the presence of Eu(III) favors HPhbH adsorption onto $\alpha,\gamma\text{-Al}_2\text{O}_3$. Janot et al. (2011, 2013) showed that Eu(III) increased adsorption of Purified Aldrich Humic Acid (PAHA) onto $\alpha\text{-Al}_2\text{O}_3$ for high PAHA concentration ($> 20 \text{ mg}_{\text{PAHA}} \cdot \text{g}_{\text{Al}_2\text{O}_3}^{-1}$) before the Eu(III) $p\text{H}$ -edge, but the adsorption of a humic acid and a simple organic acid are barely comparable (Reiller, 2012; Reiller and Buckau, 2012). One can think about the adsorption of EuPhbH^{2+} *via* the formation of a metal bridge—

type A ternary surface complex (Schindler, 1991)—as evidenced for Pb(II)-malonic acid complex on hematite (Lenhart et al., 2001). The adsorption *via* a ligand bridged ternary surface complex— type B ternary surface complex (Schindler, 1991)—under these *pH* conditions would require the adsorption *via* the phenolic function, which is unlikely (Evanko and Dzombak, 1998; Gu et al., 1995).

The solubility trend in the $\alpha,\gamma\text{-Al}_2\text{O}_3$ particles evidenced in Moreau et al. (2013) for the $\alpha,\gamma\text{-Al}_2\text{O}_3$ binary system is not modified in the $\text{Eu(III)/HPhbH}/\alpha,\gamma\text{-Al}_2\text{O}_3$ ternary system (Fig. S11 of the SI).

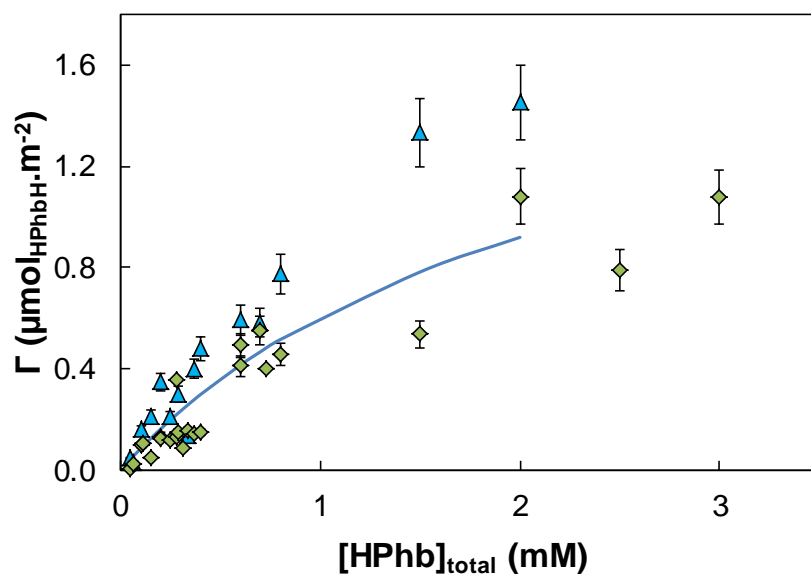


Fig. 7. Adsorption of HPhbH onto $\alpha,\gamma\text{-Al}_2\text{O}_3$ in HPhbH/ $\alpha,\gamma\text{-Al}_2\text{O}_3$ binary system (green diamonds from Moreau et al., 2013) and $\text{Eu(III)/HPhbH}/\alpha,\gamma\text{-Al}_2\text{O}_3$ ternary system (blue triangles, this study). Experimental conditions: $C(\alpha,\gamma\text{-Al}_2\text{O}_3) = 0.5 \text{ g L}^{-1}$, *pH* 5, *I* = 10 mM, in ternary system $[\text{Eu(III)}] = 10 \text{ }\mu\text{M}$. Error bars represent experimental uncertainty. Simulation without ternary complexes (blue line) of the experimental points of the $\text{Eu(III)/HPhbH}/\alpha,\gamma\text{-Al}_2\text{O}_3$ ternary system (triangles) using FITEQL 4.0 (plain line).

Conversely, as shown in Fig. 8, the amount of adsorbed Eu(III) in the ternary system is close to that adsorbed in the Eu(III)/ α,γ -Al₂O₃ binary system. It means that the presence of HPhbH does not modify the amount of adsorbed Eu(III). However the uncertainty of experimental data in the Eu(III)/HPhbH/ α,γ -Al₂O₃ ternary system increases as the concentration of HPhbH increases (Fig. 8). At pH 5, adsorption of HPhbH onto α,γ -Al₂O₃ is achieved only through the carboxylate group, as already discussed by Moreau et al. (2013). Formation of EuPhbH²⁺ complex is also achieved *via* the carboxylate group of HPhbH (PhbH⁻) (Moreau et al., 2015). Adsorbed PhbH⁻ would not likely further complex Eu(III). This could explain the constant amount of adsorbed Eu(III) whatever the total HPhbH concentration. For higher pH values the deprotonation of the phenolic oxygen—formation of Phb²⁻—could lead to an increase of the amount of adsorbed Eu(III). Alliot et al. (2006) showed that in the low acetate and carbonate concentration range, *i.e.*, below 10 mM, the amount of adsorbed Eu(III) onto α,γ -Al₂O₃ is constant.

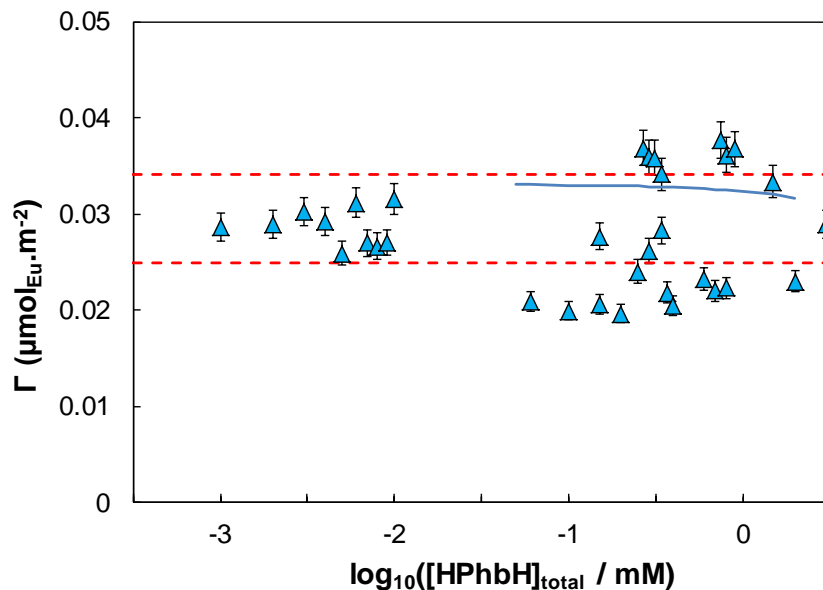


Fig. 8. Adsorption of Eu(III) onto $\alpha,\gamma\text{-Al}_2\text{O}_3$ in Eu(III)/ $\alpha,\gamma\text{-Al}_2\text{O}_3$ binary system (red dotted lines, range determined with 4 independent experiments) and in Eu(III)/Phb/ $\alpha,\gamma\text{-Al}_2\text{O}_3$ ternary system (triangles). $[\text{Eu(III)}] = 10 \mu\text{M}$, $C(\alpha,\gamma\text{-Al}_2\text{O}_3) = 0.5 \text{ g L}^{-1}$, $p\text{H } 5$, $I = 10 \text{ mM NaCl}$. Error bars represent experimental uncertainty. Fitted points using FITEQL 4.0 (plain line)

3.2.3. Modelling of the Eu(III)/HPhbH/ $\alpha,\gamma\text{-Al}_2\text{O}_3$ ternary system

Fitting the data with FITEQL 4.0 software is attempted in order to describe the interactions, and possibly determine an adsorption constant for the ternary complex previously evidenced with TRLS. First, the data are fitted assuming that the ternary system can be described as a sum of the different binary systems. Moreover, the following assumptions are made: (i) Eu^{3+} can adsorb onto $\equiv\text{YOH}$ and $\equiv\text{XOH}$ sites previously described with adsorption constants from Table 2; (ii) HPhbH can adsorb onto $\equiv\text{YOH}$ and $\equiv\text{XOH}$ sites with the adsorption constant— $\log_{10}K_{\text{sor},\text{HPhbH}} = 3.4$ within the constant capacitance model (Moreau et al., 2013); and (iii) formation of EuPhbH^{2+} in solution using the complexation constant determined in Moreau et al. (2015). One can remind that the PZSE obtained by titration for CCM, and IEP obtained by

ζ -potential for DLM, were not the same in Moreau et al. (2013) evidencing specific adsorption, which was not accounted for in our operational approach.

The amount of adsorbed HPhbH is underestimated by simulations using these hypotheses (Fig. 7), while the amount of adsorbed Eu(III) is well fitted (Fig. 8); note that the calculation shows that the amount of adsorbed Eu(III) is expected to slightly decrease for the highest $[\text{HPhbH}]_{\text{total}}$, which is not observed in our experiment either because of the high data uncertainty or because of the presence of a ternary complex, evidenced spectroscopically, and resulting in adsorption of EuPhbH^{2+} onto $\alpha,\gamma\text{-Al}_2\text{O}_3$. However, determining an adsorption constant for this complex is not possible because the decrease is too small. To do so, one could imagine working with higher $[\text{HPhbH}]_{\text{total}}$.

3.3. Ternary Eu(III)/HProtoH₂/ $\alpha,\gamma\text{-Al}_2\text{O}_3$ system

3.3.1. Spectroscopic results for Eu(III)

The asymmetry ratios and decay times in the Eu(III)/HProtoH₂/ $\alpha,\gamma\text{-Al}_2\text{O}_3$ ternary system are compared to those of the binary systems and free Eu(III) in Fig. 9. For the Eu(III)/HProtoH₂/ $\alpha,\gamma\text{-Al}_2\text{O}_3$ ternary system, both asymmetry ratios and decay times are very close to those obtained for binary Eu(III)/HProtoH₂ aqueous system. Only data uncertainty is slightly higher in Eu(III)/HProtoH₂/ $\alpha,\gamma\text{-Al}_2\text{O}_3$ ternary system. This means that the chemical environment of Eu(III) in the ternary system is very similar to that in the Eu(III)/HProtoH₂ binary system. In particular, only mono-exponential decays are evidenced in the Eu(III)/HProtoH₂/ $\alpha,\gamma\text{-Al}_2\text{O}_3$ ternary system due to the very low uptake of Eu(III) directly onto $\alpha,\gamma\text{-Al}_2\text{O}_3$, as is already the case in binary Eu(III)/ $\alpha,\gamma\text{-Al}_2\text{O}_3$ system—*vide ante*. However, because of the decrease in decay time as a function of $[\text{HProtoH}_2]_{\text{total}}$, it is not possible to more precisely characterize Eu(III) speciation—particularly the eventual formation of a

surface complex as for $\text{Eu(III)/HPhbH}/\alpha,\gamma\text{-Al}_2\text{O}_3$ ternary system —, the TRLS signal being too weak after a 100 μs delay.

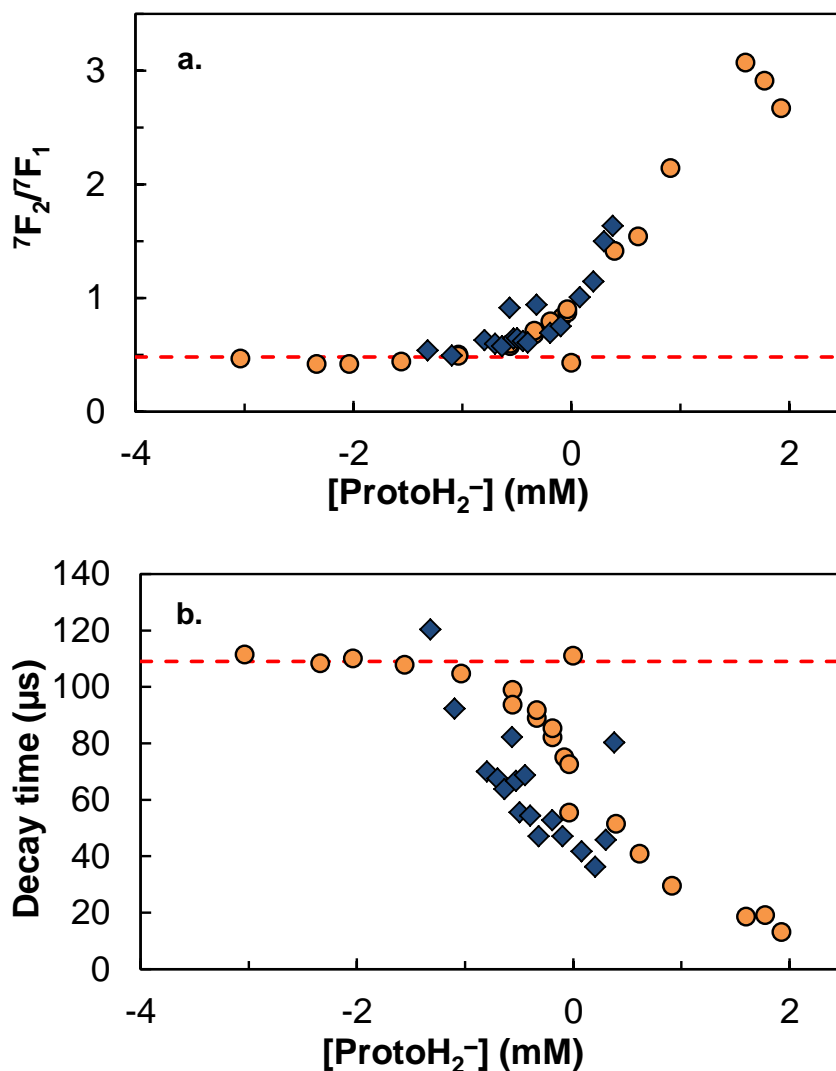


Fig. 9. Asymmetry ratios (${}^7\text{F}_2/{}^7\text{F}_1$) (a) and decay times (b) of free Eu(III) (dashed line, data for binary $\text{Eu(III)}/\alpha,\gamma\text{-Al}_2\text{O}_3$), $\text{Eu(III)}/\text{HProtoH}_2$ (circles) (Moreau et al., 2015) and ternary $\text{Eu(III)}/\text{HProtoH}_2/\alpha,\gamma\text{-Al}_2\text{O}_3$ (diamonds). $I = 10$ mM NaCl, free Eu(III) , $\text{Eu(III)}/\alpha,\gamma\text{-Al}_2\text{O}_3$, $\text{Eu(III)}/\text{HProtoH}_2/\alpha,\gamma\text{-Al}_2\text{O}_3$: $C(\alpha,\gamma\text{-Al}_2\text{O}_3) = 0.5$ g L^{-1} , $[\text{Eu(III)}] = 10$ μM , $p\text{H } 5$. $\text{Eu(III)}/\text{HProtoH}_2$: $[\text{Eu(III)}] = 1$ μM , $p\text{H } 5.5$ (Moreau et al., 2015).

3.3.2. Adsorption of HProtoH₂ and Eu(III)

Adsorption isotherms at pH 5 of HProtoH₂ onto α,γ -Al₂O₃ in the HProtoH₂/ α,γ -Al₂O₃ binary system obtained by Moreau et al. (2013) and Eu(III)/HProtoH₂/ α,γ -Al₂O₃ ternary systems are shown in Fig. 10. Adsorption of HProtoH₂ is slightly higher in the ternary system than in the HProtoH₂/ α,γ -Al₂O₃ binary system. Again, this means that the presence of Eu(III) slightly favors HProtoH₂ adsorption onto α,γ -Al₂O₃, however to a smaller extent compared to HPhbH. Concerning Eu(III) adsorption (Fig. 11), up to [HProtoH₂]_{total} = 0.4 mM the amount of adsorbed Eu(III) is of the same order of magnitude both in the Eu(III)/HProtoH₂/ α,γ -Al₂O₃ ternary system and in the Eu(III)/ α,γ -Al₂O₃ binary system. For [HProtoH₂]_{total} > 0.6 mM, the amount of adsorbed Eu(III) seems to slightly increase. This would indicate the formation of a ternary surface complex that could not be evidenced by TRLS.

As for the Eu(III)/HPhbH/ α,γ -Al₂O₃ ternary systems, the solubility of α,γ -Al₂O₃ particles in the Eu(III)/HProtoH₂/ α,γ -Al₂O₃ ternary systems is not modified compared to HPhbH/ α,γ -Al₂O₃ binary systems studied by Moreau et al. (2013)—see Fig. S12 of the SI.

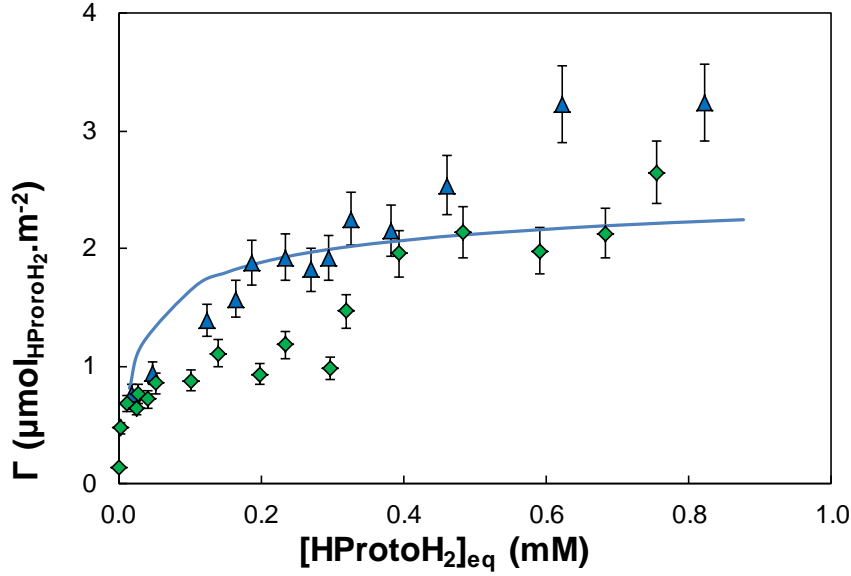
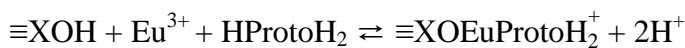


Fig. 10. Adsorption isotherms of HProtoH₂ onto 0.5 g.L⁻¹ α,γ-Al₂O₃ at pH 5 and *I* = 10 mM NaCl, in HProtoH₂/α,γ-Al₂O₃ binary system (Moreau et al., 2013) (diamonds), and in Eu(III)/HProtoH₂/α,γ-Al₂O₃ ternary system, [Eu(III)] = 10 μM (triangles). Error bars represent experimental uncertainty; Simulation of the experimental point of the Eu(III)/HProtoH₂/α,γ-Al₂O₃ ternary system using FITEQL 4.0 (plain thick line).

3.3.3. Modelling of the Eu(III)/HProtoH₂/α,γ-Al₂O₃ system

Fitting is performed using FITEQL 4.0 using the same hypotheses and using $\log_{10}K_{sorb,HProtoH_2} = 5.4$ within CCM (Moreau et al., 2013). Considering the ternary system as the sum of the binary systems does not permit to describe the increase in Eu(III) adsorption for $[HProtoH_2]_{total} > 0.6$ mM and the amount of adsorbed HProtoH₂ is slightly underestimated (Fig. 10). As a consequence, and even if the surface complex is not evidenced spectroscopically, EuProtoH₂²⁺ is assumed to adsorb also on α,γ-Al₂O₃ surface sites following:



$$K_{sorb,EuProtoH_2^{2+}} = \exp\left(-\frac{2F\psi_0}{RT}\right) \times \frac{[\equiv XOEuProtoH_2^+][H^+]^2}{[\equiv XOH^+][Eu^{3+}][HProtoH_2]} \quad (2)$$

This surface species does not permit to describe the whole data set either. Indeed, as shown in Fig. 11, even for $\log_{10}K_{\text{sorb,EuProtoH}_2^{2+}} = -0.2$, adsorption of Eu(III) is overestimated at the lower HProtoH₂ concentration. This evidences again a synergetic effect between Eu(III) and HProtoH₂ for adsorption but further information about speciation is very difficult to obtain in this work. Further experiments are needed.

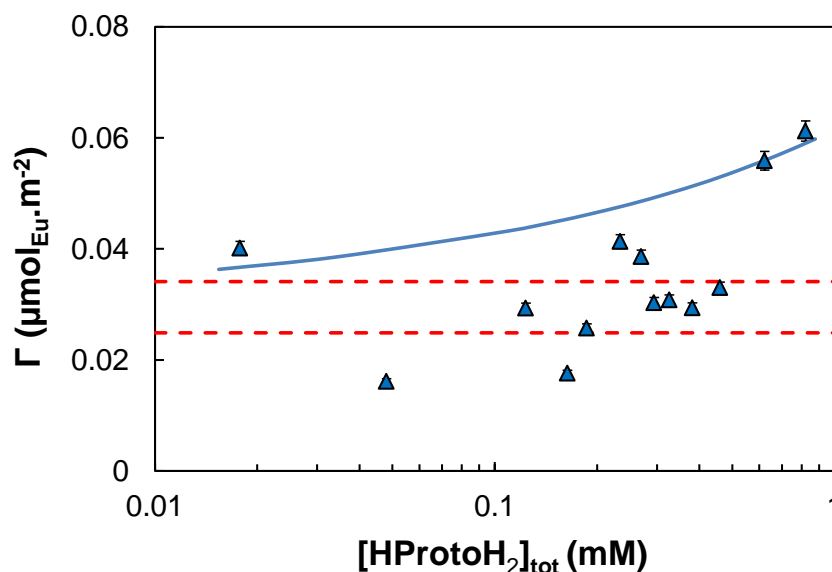


Fig. 11. Adsorption of Eu(III) in Eu(III)/ α,γ -Al₂O₃ binary system (dashed lines, the range representing the mean values of 4 independent experiments) and in Eu(III)/HProtoH₂/ α,γ -Al₂O₃ ternary system (triangles). $C(\alpha,\gamma\text{-Al}_2\text{O}_3) = 0.5 \text{ g L}^{-1}$, $[\text{Eu(III)}] = 10 \text{ }\mu\text{M}$, $p\text{H } 5$, $I = 10 \text{ mM NaCl}$; fitting using FITEQL 4.0 (plain thick line).

Finally, one could imagine that, as for the Eu(III)/HPhbH/ α,γ -Al₂O₃ ternary system, both Eu³⁺ and ProtoH₂⁻ are adsorbed onto α,γ -Al₂O₃, and that adsorption of HProtoH₂ mainly occurs *via* the carboxylate group, as in binary systems. This is consistent with the fact that, for low total HProtoH₂ concentrations, adsorption of Eu(III) in the ternary system is close to that in the Eu(III)/ α,γ -Al₂O₃ binary system but also that adsorption of HProtoH₂ in the ternary system is close to that in HProtoH₂/ α,γ -Al₂O₃ binary system. Of course, EuProtoH₂²⁺ is also formed in solution, involving the carboxylate group (Moreau et al., 2015). One can also imagine that for

the highest $[\text{HProtoH}_2]_{\text{total}}$, adsorption of EuProtoH_2^{2+} takes place involving the catechol group—type B ternary complex (Schindler, 1991)—explaining the increase of the amount of both Eu(III) and HProtoH₂ onto $\alpha,\gamma\text{-Al}_2\text{O}_3$. The small influence of HProtoH₂ on Eu(III) adsorption on $\alpha,\gamma\text{-Al}_2\text{O}_3$ is consistent with results obtained otherwise by Davis and Leckie (1978) on the Cu(II)/HProtoH₂/ferrihydrite system. Although in our case, the spectroscopic results show that the presence of an organic ligand is important from the metal speciation point of view.

4. DISCUSSIONS

4.1. Binary Eu(III)/ $\alpha,\gamma\text{-Al}_2\text{O}_3$ system

In the binary Eu(III)/ $\alpha,\gamma\text{-Al}_2\text{O}_3$ system, the spectral modifications ($D = 10 \mu\text{s}$) appears at pH values above 6.15 (Fig. S2a of the SI), i.e. when the adsorption of Eu(III) strongly increases (Fig. 3). The increase of the non-degenerated ${}^5\text{D}_0 \rightarrow {}^7\text{F}_0$ transition evidencing the loss of centro-symmetry around Eu(III) (Bünzli, 1989) as adsorption occurs. The broadening of the electric dipole ${}^5\text{D}_0 \rightarrow {}^7\text{F}_1$ transition was also observed by Janot et al. (2011, 2013) for the Eu(III)/ $\alpha\text{-Al}_2\text{O}_3$ binary system and seems then to be a characteristic of the Eu(III) adsorbed species on alumina surfaces. This modification also points to a modification of the symmetry around Eu(III) as adsorption occurs. It seems that at the best three components can be distinguished at pH 6.65 and 7.05 in Fig. S2a of the SI, which points to a low symmetry point group (Görller-Walrand and Binnemans, 1996) with centre of inversion, i.e. C_{2v} or lower.

Hence, the decomposition of the ${}^5\text{D}_0 \rightarrow {}^7\text{F}_0$, ${}^5\text{D}_0 \rightarrow {}^7\text{F}_1$ and ${}^5\text{D}_0 \rightarrow {}^7\text{F}_2$ transitions from the spectrum obtained at pH 7.05 with respectively one, three, and four Lorentzian-Gaussian peaks (McNemar and Horrocks, 1989; Reiller et al., 2011)

$$F_i = F_{\max,i} \frac{\exp\left[-0.5 \left(\frac{\lambda_i - \lambda_{\max,i}}{\sigma_i}\right)^2\right]}{\left(\frac{\lambda_i - \lambda_{\max,i}}{\sigma_i}\right)^2 + 1} \quad (3)$$

between 570 nm and 630 nm is presented in Fig. S2b of the SI—see fitting parameters and correlation matrices in Table S6 of the SI. The highest uncertainties in the fitting parameters are on the maximum intensity of the third and fourth components of the $^5D_0 \rightarrow ^7F_2$ transition, which are also showing the highest correlation. The maximum of the $^5D_0 \rightarrow ^7F_0$, $^5D_0 \rightarrow ^7F_1$ and $^5D_0 \rightarrow ^7F_2$ transitions are 578.7, 591.5, and 615.9 nm, respectively. The assignment to Stark levels would require low temperature experiments.

The obtained values for the asymmetry ratio in this study (Fig. 2a) are consistent with the data from Rabung et al. (2000) and Janot et al. (2011). The influence of ionic strength, in the range 10–100 mM is very limited, which was already observed by Janot et al. (2011, 2013). However, Rabung et al. (2000) found that $^7F_2/^7F_1$ kept increasing even for *pH* values above 7. Note that in this work, as well as in Janot et al. (2011, 2013), $^7F_2/^7F_1$ values are determined using peak areas whereas Rabung et al. (2000) used the intensity at two maxima wavelengths (594 and 619 nm). It is also worthwhile noting that our experimental set up is the same as the one in Janot et al. (2011, 2013), *i.e.*, a spectrometer equipped with a 600 lines/mm grating, whereas Rabung et al. (2000) used a 300 lines/nm grating. In the latter case, the convolution with the spectrometer is more important, leading to broader peaks with a slightly lower intensity (Brevet et al., 2009; de Levie, 2005). This is particularly important in the case of high *pH* data in Rabung et al. (2000)

For Eu(III)/ α,γ -Al₂O₃ binary system at *pH* 4.7 (Fig. S3 of the SI) a mono-exponential decay is obtained (Table S7 of the SI). This value is not different from that of free Eu³⁺ obtained by Moreau et al. (2015). Concurrently, the spectrum recorded for *D* = 10 μ s and *pH* 4.7 is not modified compared to free Eu³⁺, which is a consequence of the small amount of adsorbed

Eu(III) (see Fig. 3) that cannot be evidenced by TRLS. The inset to Fig. S3 of the SI is also showing that the spectrum is not modified at higher delay. The main contribution to the TRLS signal, in the Eu(III)/ α,γ -Al₂O₃ binary system at pH 4.7 is due to free Eu³⁺.

Fig. S4 of the SI is showing that decay at pH 5.25 is not perfectly mono-exponential— $\tau = 121 \pm 1 \mu\text{s}$ —, but the fitting procedure does not permit to obtain satisfactory bi-exponential decay— $\tau_1 = (117 \pm 2) \mu\text{s}$ and $\tau_2 = (605 \pm 908) \mu\text{s}$ —because of a lack of signal at $D > 550 \mu\text{s}$, and due to the small amount of adsorbed Eu³⁺ (see Fig. 3). The reported value of decay time in Fig. 2b for pH 5.25 is the one determined in Fig. S4 of the SI with mono-exponential fitting—*vide supra*. It is slightly higher than for Eu³⁺, evidencing that the amount of adsorbed Eu(III) increases from pH 4.7 to pH 5.25, which is consistent with the increasing amount of adsorbed Eu(III) with pH (Fig. 3). The application of the operational relationship proposed by Kimura and Choppin (1994), justified in Polly et al. (2013; 2010) yields to the loss of one water molecule in the first hydration sphere for τ and τ_1 , respectively (Table S7 of the SI). This may indicate the loss of one water molecule in the case of our α,γ -Al₂O₃ sample, but this value can be biased by the poor quality of the fit. Takahashi et al. (2000) proposed that the surface complex formed at pH 5 with montmorillonite is of an outer sphere type, meaning that adsorption occurs *via* the second hydration sphere of Eu(III), and that the decay time is not significantly different from that of free Eu³⁺; only spectra of Eu(III) adsorbed onto montmorillonite and of Eu(H₂O)_n³⁺ are slightly different. Here the Eu(III) spectrum is showing only minor differences, and decay time would point to a species that is adsorbed as a monodentate. The inset to Fig. S4 of the SI is showing the spectra normalized to the total wavelength span at $D = 10 \mu\text{s}$ and at $D = 650 \mu\text{s}$. This indicates that a second species, with a longer decay time is occurring in the system, which decay time, and hydration, cannot be resolved.

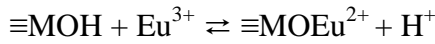
At pH 6.15, a bi-exponential decay is clearly evidenced in Fig. S5 of the SI—repartition of the residuals and correlation matrices in Table S3 of the SI. This differs from Rabung et al. (2000) and Janot et al. (2011, 2013), who found mono-exponential decays at this pH value. The short decay time of the fast decaying component (Table S7 of the SI) obtained in this study is not significantly different from that of free Eu^{3+} —typically 110 μs (Horrocks and Sudnick, 1979)—, which indicates an outer-sphere complex. The slow decay value is very close to that obtained by Janot et al. (2011, 2013) at this pH for $I = 10$ mM. The loss of five water molecules in the first hydration sphere for the slow decaying component is pointing to the formation of a multidentate species. The modification of the luminescence spectra with delay is evidenced in the inset to Fig. S5 of the SI at $D = 790$ μs . These results are consistent with the formation of an inner sphere multidentate complex between $Eu(III)$ and $\alpha,\gamma-Al_2O_3$ surface sites, as pH increases because both spectrum and decay time are modified (Janot et al., 2011, 2013; Rabung et al., 2000). The formation of an hydrolyzed multidentate surface complex, i.e. $\equiv AlOEu(OH)^+$, is also possible.

For the similar spectra obtained at pH 6.65 (Fig. S6a of the SI) and 7.05 (Fig. S7b a of the SI), similar bi-exponential decays are observed (Table S7 of the SI). Neither Rabung et al. (2000) nor Janot et al. (2011, 2013) evidenced bi-exponential decay times for their $Eu(III)/Al_2O_3$ binary system even above pH 7. However, the obtained values for the short-lived component are very close to that obtained by Janot et al. (2011) in this pH range with $I = 10$ mM NaCl. The loss of *approx.* 3 and 6 water molecules in the first hydration sphere also points to the formation of multidentate surface species (Polly et al., 2013; Polly et al., 2010).

In our case, the observed bi-exponential decays could evidence the two different types of sites previously proposed here and by others for different oxides (Bargar et al., 1997; Rabung et al., 2000). The comprehensive description of spectra and determination of all adsorbed or dissolved $Eu(III)$ species is not possible because of the complexity of $Eu(III)$ speciation for pH

values above 6 as Eu(III) carbonate and hydroxide complexes are present. To further elucidate Eu(III) speciation in such a case, it would be necessary to perform experiments under a carbonate-free atmosphere.

In a first attempt, the modelling of the *pH*-isotherm is performed using the constant capacitance model (CCM) and double layer model (DLM) with FITEQL 4.0 software (Herbelin and Westall, 1994), using oxide characteristics determined in Moreau et al. (2013) and recalled in Table 2. First, only one adsorption equilibrium is considered:



$$K_{\text{sorb,Eu}^{3+}} = \exp\left(-\frac{\Delta z F \psi_0}{RT}\right) \frac{[\equiv\text{MOEu}^{2+}] [\text{H}^+]}{[\equiv\text{MOH}] [\text{Eu}^{3+}]} = \exp\left(-\frac{2F\psi_0}{RT}\right) \frac{[\equiv\text{MOEu}^{2+}] [\text{H}^+]}{[\equiv\text{MOH}] [\text{Eu}^{3+}]} \quad (4)$$

The parameters obtained using CCM and DLM are presented in Table 2 and lead to very similar fitting quality as shown in Fig. 3. Adsorption constants obtained with CCM and DLM are showing different values ($\log_{10}K_{\text{sorb,Eu}^{3+}} = 2.3 \pm 0.1$ for CCM and $\log_{10}K_{\text{sorb,Eu}^{3+}} = 4.9 \pm 0.2$ for DLM) because of the difference in the oxide characteristics for both models—see Moreau et al. (2013) for details. The fitting curves, shown in Fig. 3 (dashed lines), are in very good agreement for *pH* > 6, but for lower *pH* values the fitting underestimates the adsorption of Eu(III).

Hence, data are fitted using CCM and DLM models with two adsorption sites of different energies: $\equiv\text{XOH}$ and $\equiv\text{YOH}$. This could be due to the presence of two crystalline phases (or faces) of the oxide: $\alpha\text{-Al}_2\text{O}_3$ and $\gamma\text{-Al}_2\text{O}_3$, in the amount 15% and 85% respectively. The acidities of both sites are considered to have the same protolytic properties because only one amphoteric site is evidenced by potentiometric titration by Moreau et al. (2013).





In order to determine the adsorption constants for both adsorption sites $\equiv\text{XOH}$ and $\equiv\text{YOH}$, data corresponding to $\text{pH} > 6$ are first fitted to determine $\log_{10}K_{\text{X,Eu}^{3+}}$ and $[\equiv\text{XOH}]$ then a second fitting procedure is done on all data to determine $\log_{10}K_{\text{Y,Eu}^{3+}}$ and $[\equiv\text{YOH}]$. The results obtained using CCM and DLM are presented in Table 2 and lead to very similar fit quality (Fig. 3). The fitting curves are in very good agreement for the whole pH range and one can conclude that adsorption of Eu(III) onto the studied $\alpha,\gamma\text{-Al}_2\text{O}_3$ involves two adsorption sites. The adsorption constants determined in this work are higher than those determined otherwise for adsorption onto hematite of Eu(III) (Rabung et al., 1998b), and La(III) (Marmier and Fromage, 1999). However, the value determined in this work corresponding to adsorption of Eu(III) onto the lowest affinity site for Eu(III) ($\equiv\text{YOH}$) is in the same order of magnitude as the one of the adsorption site determined by Rabung et al. (1998b).

It seems then that both spectroscopic and macroscopic data are pointing to (at the least) two adsorption sites on our $\alpha,\gamma\text{-Al}_2\text{O}_3$ sample. Nevertheless, the density of the sites, suggested by the decay times analyses, are not represented in the modelling. One would have to account for the nature of surface sites (Hiemstra et al., 1989), which is not possible with our modelling strategy.

4.2. Ternary Eu(III)/HPhbH/ $\alpha,\gamma\text{-Al}_2\text{O}_3$ system

In the ternary Eu(III)/HPhbH/ $\alpha,\gamma\text{-Al}_2\text{O}_3$ system both the increase in the ${}^5\text{D}_0 \rightarrow {}^7\text{F}_0$ and the ${}^5\text{D}_0 \rightarrow {}^7\text{F}_2$ transitions are evidencing the change in symmetry upon adsorption (Fig. 4). The loss of centro-symmetry around Eu(III) is clearly shown by the ${}^5\text{D}_0 \rightarrow {}^7\text{F}_0$ (Bünzli, 1989), but contrary to the binary Eu(III)/ $\alpha,\gamma\text{-Al}_2\text{O}_3$ system at higher pH , no substructure can be evidenced

in the ${}^5D_0 \rightarrow {}^7F_1$ transition. The chemical environment of Eu(III) has changed upon complexation by PhbH⁻ and/or adsorption onto α,γ -Al₂O₃, in the ternary system.

5. CONCLUSION

Our aim is to study the interactions occurring in a system containing three entities, *i.e.* Eu(III), a hydrobenzoic acid and α,γ -Al₂O₃ particles, in order to determine whether the acids modify adsorption and speciation of Eu(III). We have evidenced synergetic processes for adsorption of Eu(III) and hydrobenzoic acids onto α,γ -Al₂O₃. For the two ternary systems studied, adsorption of the acids is higher than for the corresponding acid/ α,γ -Al₂O₃ binary systems. Dissolution of α,γ -Al₂O₃ is not enhanced in the ternary systems as compared to acid/ α,γ -Al₂O₃ binary systems previously studied by Moreau et al. (2013). Eu(III) adsorption is not increased in the Eu(III)/HPhbH/ α,γ -Al₂O₃ ternary system as compared to the Eu(III)/ α,γ -Al₂O₃ binary system. Ternary surface species involving alumina surface site, Eu(III), and HPhbH is characterized at the highest HPhbH total concentrations. A spectroscopic fingerprint of this species can be recorded because the decay time of Eu(III) in this species is higher than 110 μ s. Adsorption of Eu(III) is increased in the Eu(III)/HProtoH₂/ α,γ -Al₂O₃ ternary system as compared to Eu(III)/ α,γ -Al₂O₃ binary system. However, a comprehensive description of the Eu(III)/HProtoH₂/ α,γ -Al₂O₃ ternary system by TRLS is not possible because of the weak luminescence signal as decay time of Eu(III) in binary or ternary species decreases with increasing HProtoH₂ total concentration.

The simulation of the data shows that adsorption of EuProtoH₂²⁺ has to be taken into account to describe the increased adsorption of Eu(III) for high HProtoH₂ concentrations. To further elucidate the surface complexes that are formed in the Eu(III)/HProtoH₂/ α,γ -Al₂O₃ ternary system, it could be interesting to study the ternary system involving catechol as it would permit to discriminate between two factors: (i) between the role of carboxylate and catechuic

groups; and (ii) to elucidate if complexation between Eu(III) and HProtoH₂ in the Eu(III)/HProtoH₂/ α,γ -Al₂O₃ ternary system could be achieved *via* the catechuic group.

ACKNOWLEDGEMENT.

This work was supported by the RSTB program (RBPCH project) from CEA, and the French Direction Générale de l'Armement (DGA). Dr Thomas Rabung is acknowledged for providing its original TRLS data for Eu(III)/ γ -Al₂O₃ system. Camille Auriault is acknowledged for her help in experimental work. Michel Tabarant and Hawa Badji (CEA/DEN/DANS/SEARS/LISL) are acknowledged for their help and assistance during the ICP-OES measurements.

REFERENCES

Alliot, C., Bion, L., Mercier, F., Toulhoat, P., 2006. Effect of aqueous acetic, oxalic, and carbonic acids on the adsorption of europium(III) onto α -alumina. J. Colloid Interface Sci. 298, 573-581, <http://dx.doi.org/10.1016/j.jcis.2006.01.004>.

Alliot, C., Bion, L., Mercier, F., Vitorge, P., Toulhoat, P., 2005a. Effect of aqueous acetic, oxalic and carbonic acids on the adsorption of americium onto α -alumina. Radiochim. Acta 93, 435-442, <http://dx.doi.org/10.1524/ract.2005.93.8.435>.

Alliot, C., Vitorge, P., Bion, L., Mercier, F., 2005b. Effect of aqueous acetic, oxalic and carbonic acids on the adsorption of uranium(VI) onto α -alumina. New J. Chem. 29, 1409-1415, <http://dx.doi.org/10.1039/b508353b>.

Aoyagi, N., Toraiishi, T., Geipel, G., Hotokezaka, H., Nagasaki, S., Tanaka, S., 2004.

Fluorescence characteristics of complex formation of europium(III)-salicylate. Radiochim. Acta 92, 589-593, <http://dx.doi.org/10.1524/ract.92.9.589.54997>.

Aydin, R., Özer, U., 2004. Potentiometric and spectroscopic studies on yttrium(III) complexes of dihydroxybenzoic acids. *Chem. Pharm. Bull.* 52, 33-37,

<http://dx.doi.org/10.1248/cpb.52.33>.

Bargar, J.R., Towle, S.N., Brown, G.E., Jr., Parks, G.A., 1997. XAFS and bond-valence determination of the structures and compositions of surface functional groups and Pb(II) and Co(II) sorption products on single-crystal α -Al₂O₃. *J. Colloid Interface Sci.* 185, 473-492,

<http://dx.doi.org/10.1006/jcis.1996.4574>.

Binnemans, K., Jones, P.T., Van Acker, K., Blanpain, B., Mishra, B., Apelian, D., 2013.

Rare-earth economics: the balance problem. *JOM* 65, 846-848,

<http://dx.doi.org/10.1007/s11837-013-0639-7>.

Bourg, A.C.M., Schindler, P.W., 1978. Ternary surface complexes. 1. Complex-formation in system silica-Cu(II)-ethylenediamine - Preliminary communication. *Chimia* 32, 166-168.

Bradbury, M.H., Baeyens, B., 2005. Modelling the sorption of Mn(II), Co(II), Ni(II), Zn(II), Cd(II), Eu(III), Am(III), Sn(IV), Th(IV), Np(V) and U(VI) on montmorillonite: linear free energy relationships and estimates of surface binding constants for some selected heavy metals and actinides. *Geochim. Cosmochim. Acta* 69, 875-892,

<http://dx.doi.org/10.1016/j.gca.2004.07.020>.

Bradbury, M.H., Baeyens, B., 2009a. Sorption modelling on illite Part I: titration measurements and the sorption of Ni, Co, Eu and Sn. *Geochim. Cosmochim. Acta* 73, 990-1003, <http://dx.doi.org/10.1016/j.gca.2008.11.017>.

Bradbury, M.H., Baeyens, B., 2009b. Sorption modelling on illite. Part II: actinide sorption and linear free energy relationships. *Geochim. Cosmochim. Acta* 73, 1004-1013,

<http://dx.doi.org/10.1016/j.gca.2008.11.016>.

Brevet, J., Claret, F., Reiller, P.E., 2009. Spectral and temporal luminescent properties of Eu(III) in humic substance solutions from different origins. *Spectrochim. Acta, Part A* 74, 446-453, <http://dx.doi.org/10.1016/j.saa.2009.06.042>.

Bünzli, J.-C.G., 1989. Luminescent Probes, in: Bünzli, J.-C.G., Choppin, G.R. (Eds.), *Lanthanides Probes in Life, Chemical and Earth Sciences – Theory and Practice*. Elsevier, Amsterdam.

Carnall, W.T., Fields, P.R., Rajnak, K., 1968. Electronic energy levels of trivalent lanthanide aquo ions. IV. Eu^{3+} . *J. Chem. Phys.* 49, 4450-4455, <http://dx.doi.org/10.1063/1.1669896>.

Censi, P., Randazzo, L.A., D'Angelo, S., Saiano, F., Zuddas, P., Mazzola, S., Cuttitta, A., 2013. Relationship between lanthanide contents in aquatic turtles and environmental exposures. *Chemosphere* 91, 1130-1135, <http://dx.doi.org/10.1016/j.chemosphere.2013.01.017>.

Claret, F., Schäfer, T., Brevet, J., Reiller, P.E., 2008. Fractionation of Suwannee River fulvic acid and aldrich humic acid on $\alpha\text{-Al}_2\text{O}_3$: spectroscopic evidence. *Environ. Sci. Technol.* 42, 8809-8815, <http://dx.doi.org/10.1021/Es801257g>.

Claret, F., Schäfer, T., Rabung, T., Wolf, M., Bauer, A., Buckau, G., 2005. Differences in properties and Cm(III) complexation behavior of isolated humic and fulvic acid derived from Opalinus clay and Callovo-Oxfordian argillite. *Appl. Geochem.* 20, 1158-1168, <http://dx.doi.org/10.1016/j.apgeochem.2005.01.008>.

Davis, J.A., Leckie, J.O., 1978. Effect of adsorbed complexing ligands on trace-metal uptake by hydrous oxides. *Environ. Sci. Technol.* 12, 1309-1315, <http://dx.doi.org/10.1021/es60147a006>.

de Levie, R., 2005. *Advanced Excel for Scientific Data Analysis*. Oxford University Press.

- Dobbs, J.C., Susetyo, W., Knight, F.E., Castles, M.A., Carreira, L.A., Azarraga, L.V., 1989. Characterization of metal-binding sites in fulvic acids by lanthanide ion probe spectroscopy. *Anal. Chem.* 61, 483-488, <http://dx.doi.org/10.1021/ac00180a020>.
- Evanko, C.R., Dzombak, D.A., 1998. Influence of structural features on sorption of NOM-analogue organic acids to goethite. *Environ. Sci. Technol.* 32, 2846-2855, <http://dx.doi.org/10.1021/es980256t>.
- Furrer, G., Stumm, W., 1986. The coordination chemistry of weathering: I. Dissolution kinetics of δ -Al₂O₃ and BeO. *Geochim. Cosmochim. Acta* 50, 1847-1860, [http://dx.doi.org/10.1016/0016-7037\(86\)90243-7](http://dx.doi.org/10.1016/0016-7037(86)90243-7).
- Görller-Walrand, C., Binnemans, K., 1996. Rationalization of crystal-field parametrization, in: Gschneidner, K.A., Jr., Eyring, L. (Eds.), *Handbook on the Physics and Chemistry of Rare Earths*. Elsevier, pp. 121-283.
- Gu, B., Schmitt, J., Chen, Z., Liang, L.Y., McCarthy, J.F., 1995. Adsorption and desorption of different organic matter fractions on iron oxide. *Geochim. Cosmochim. Acta* 59, 219-229, [http://dx.doi.org/10.1016/0016-7037\(94\)00282-Q](http://dx.doi.org/10.1016/0016-7037(94)00282-Q).
- Guo, Z.J., Yu, X.M., Guo, F.H., Tao, Z.Y., 2005. Th(IV) adsorption on alumina: effects of contact time, pH, ionic strength and phosphate. *J. Colloid Interface Sci.* 288, 14-20, <http://dx.doi.org/10.1016/j.jcis.2005.02.056>.
- Hasegawa, Y., Morita, Y., Hase, M., Nagata, M., 1989. Complexation of lanthanoid(III) with substituted benzoic or phenylacetic acids and extraction of these acids. *Bull. Chem. Soc. Jpn.* 62, 1486-1491, <http://dx.doi.org/10.1246/bcsj.62.1486>.
- Hatzipanayioti, D., Karaliota, A., Kamariotaki, M., Aletras, V., Petropouleas, P., 2006. Theoretical and spectroscopic investigation of the oxidation and degradation of protocatechuic acid. *Chem. Phys.* 325, 341-350, <http://dx.doi.org/10.1016/j.chemphys.2005.12.029>.

Herbelin, A., Westall, J., 1994. FITEQL. A computer program for determination of chemical equilibrium constant from experimental data Version 4.0, Corvallis, Oregon, USA.

Hiemstra, T., Van Riemsdijk, W.H., Bolt, G.H., 1989. Multisite proton adsorption modeling at the solid/solution interface of (hydr)oxides: a new approach. I. Model description and evaluation of intrinsic reaction constants. *J. Colloid Interface Sci.* 133, 91-104,
[http://dx.doi.org/10.1016/0021-9797\(89\)90284-1](http://dx.doi.org/10.1016/0021-9797(89)90284-1).

Horrocks, W.D., Jr., Sudnick, D.R., 1979. Lanthanide ion probes of structure in biology. Laser-induced luminescence decay constants provide a direct measure of the number of metal-coordinated water-molecules. *J. Am. Chem. Soc.* 101, 334-340,
<http://dx.doi.org/10.1021/ja00496a010>.

Huittinen, N., Rabung, T., Lutzenkirchen, J., Mitchell, S.C., Bickmore, B.R., Lehto, J., Geckeis, H., 2009. Sorption of Cm(III) and Gd(III) onto gibbsite, α -Al(OH)₃: a batch and TRLFS study. *J. Colloid Interface Sci.* 332, 158-164,
<http://dx.doi.org/10.1016/j.jcis.2008.12.017>.

Hummel, W., Berner, U., Curti, E., Pearson, F.J., Thoenen, T., 2002. Nagra/PSI Chemical Thermodynamic Data Base 01/01. NAGRA, Parkland, FL, USA.

Janot, N., Benedetti, M.F., Reiller, P.E., 2011. Colloidal α -Al₂O₃, europium(III) and humic substances interactions: a macroscopic and spectroscopic study. *Environ. Sci. Technol.* 45, 3224-3230, <http://dx.doi.org/10.1021/es102592a>.

Janot, N., Benedetti, M.F., Reiller, P.E., 2013. Influence of solution parameters on europium(III), α -Al₂O₃ and humic acid interactions: macroscopic and time-resolved laser-induced luminescence data. *Geochim. Cosmochim. Acta* 123, 35-54,
<http://dx.doi.org/10.1016/j.gca.2013.08.038>.

Jejurkar, C.R., Mavani, I.P., Bhattacharya, P.K., 1972. Some metal-complexes with catechol, pyrogallol, 2,3-dihydroxynaphthalene and protocatechuic acid. *Indian J. Chem.* 10, 1190-1192.

Johnson, S.B., Yoon, T.H., Brown, G.E., Jr., 2005. Adsorption of organic matter at mineral/water interfaces: 5. Effects of adsorbed natural organic matter analogues on mineral dissolution. *Langmuir* 21, 2811-2821, <http://dx.doi.org/10.1021/la0481041>.

Jørgensen, C.K., Judd, B.R., 1964. Hypersensitive pseudoquadrupole transitions in lanthanides. *Mol. Phys.* 8, 281-290, <http://dx.doi.org/10.1080/00268976400100321>.

Kielland, J., 1937. Individual activity coefficients of ions in aqueous solutions. *J. Am. Chem. Soc.* 59, 1675-1678, <http://dx.doi.org/10.1021/ja01288a032>.

Kimura, T., Choppin, G.R., 1994. Luminescence study on determination of the hydration number of Cm(III). *J. Alloys Compd.* 213, 313-317, [http://dx.doi.org/10.1016/0925-8388\(94\)90921-0](http://dx.doi.org/10.1016/0925-8388(94)90921-0).

Kosmulski, M., 2009. Compilation of PZC and IEP of sparingly soluble metal oxides and hydroxides from literature. *Adv. Colloid Interface Sci.* 152, 14-25, <http://dx.doi.org/10.1016/j.cis.2009.08.003>.

Kuke, S., Marmodée, B., Eidner, S., Schilde, U., Kumke, M.U., 2010. Intramolecular deactivation processes in complexes of salicylic acid or glycolic acid with Eu(III). *Spectrochim. Acta, Part A* 75, 1333-1340, <http://dx.doi.org/10.1016/j.saa.2009.12.080>.

Kumar, S., Kar, A.S., Tomar, B.S., Bhattacharyya, D., 2012. X-ray absorption fine structure spectroscopy study of Eu(III) sorption products onto amorphous silica and gamma-alumina: effect of pH and substrate. *Polyhedron* 33, 33-40, <http://dx.doi.org/10.1016/j.poly.2011.11.009>.

- Lefèvre, G., Duc, M., Lepeut, P., Caplain, R., Fedoroff, M., 2002. Hydration of γ -alumina in water and its effects on surface reactivity. *Langmuir* 18, 7530-7537, <http://dx.doi.org/10.1021/la025651j>.
- Lenhart, J.J., Bargar, J.R., Davis, J.A., 2001. Spectroscopic evidence for ternary surface complexes in the lead(II)–malonic acid–hematite system. *J. Colloid Interface Sci.* 234, 448-452, <http://dx.doi.org/10.1006/jcis.2000.7345>.
- Marang, L., Eidner, S., Kumke, M.U., Benedetti, M.F., Reiller, P.E., 2009. Spectroscopic characterization of the competitive binding of Eu(III), Ca(II), and Cu(II) to a sedimentary originated humic acid. *Chem. Geol.* 264, 154-161, <http://dx.doi.org/10.1016/j.chemgeo.2009.03.003>.
- Marmier, N., Fromage, F., 1999. Comparing electrostatic and nonelectrostatic surface complexation modeling of the sorption of lanthanum on hematite. *J. Colloid Interface Sci.* 212, 252-263, <http://dx.doi.org/10.1006/jcis.1998.6039>.
- Marmodée, B., de Klerk, J.S., Ariese, F., Gooijer, C., Kumke, M.U., 2009. High-resolution steady-state and time-resolved luminescence studies on the complexes of Eu(III) with aromatic or aliphatic carboxylic acids. *Anal. Chim. Acta* 652, 285-294, <http://dx.doi.org/10.1016/j.aca.2009.06.006>.
- Marques Fernandes, M., Stumpf, T., Baeyens, B., Walther, C., Bradbury, M.H., 2010. Spectroscopic identification of ternary Cm-carbonate surface complexes. *Environ. Sci. Technol.* 44, 921-927, <http://dx.doi.org/10.1021/es902175w>.
- McNemar, C.W., Horrocks, W.D., Jr., 1989. The resolution of laser-induced europium(III) ion excitation-spectra through the use of the Marquardt nonlinear-regression method. *Appl. Spectrosc.* 43, 816-821, <http://dx.doi.org/10.1366/0003702894202256>.

Moermond, C.T.A., Tijink, J., Van Wezel, A.P., Koelmans, A.A., 2001. Distribution, speciation, and bioavailability of lanthanides in the Rhine-Meuse estuary, The Netherlands. *Environ. Toxicol. Chem.* 20, 1916-1926, <http://dx.doi.org/10.1002/etc.5620200909>.

Molis, E., Barrès, O., Marchand, H., Sauzéat, E., Humbert, B., Thomas, F., 2000. Initial steps of ligand-promoted dissolution of gibbsite. *Colloids Surf., A* 163, 283-292, [http://dx.doi.org/10.1016/S0927-7757\(99\)00305-2](http://dx.doi.org/10.1016/S0927-7757(99)00305-2).

Moreau, P., Colette-Maatouk, S., Gareil, P., Reiller, P.E., 2013. Modelling the adsorption of phenolic acids onto α,γ -alumina particles. *Colloids Surf., A* 435, 97-108, <http://dx.doi.org/10.1016/j.colsurfa.2013.02.035>.

Moreau, P., Colette-Maatouk, S., Vitorge, P., Gareil, P., Reiller, P.E., 2015. Complexation of europium(III) by hydroxybenzoic acids: a time-resolved luminescence spectroscopy study. *Inorg. Chim. Acta* 432, 81-88, <http://dx.doi.org/10.1016/j.ica.2015.03.036>.

Morel, J.P., Marmier, N., Hurel, C., Morel-Desrosiers, N., 2012. Effect of temperature on the sorption of europium on alumina: microcalorimetry and batch experiments. *J. Colloid Interface Sci.* 376, 196-201, <http://dx.doi.org/10.1016/j.jcis.2012.02.035>.

Pearson, R.G., 1963. Hard and soft acids and bases. *J. Am. Chem. Soc.* 85, 3533-3539, <http://dx.doi.org/10.1021/ja00905a001>.

Polly, R., Schimmelpfennig, B., Flörsheimer, M., Rabung, T., Kupcik, T., Klenze, R., Geckeis, H., 2013. Quantum chemical study of inner-sphere complexes of trivalent lanthanide and actinide ions on the corundum (110) surface. *Radiochim. Acta* 101, 561-570, <http://dx.doi.org/10.1524/ract.2013.2054>.

Polly, R., Schimmelpfennig, B., Rabung, T., Flörsheimer, M., Klenze, R., Geckeis, H., 2010. Quantum chemical study of inner-sphere complexes of trivalent lanthanide and actinide ions on the corundum (0001) surface. *Radiochim. Acta* 98, 627-634, <http://dx.doi.org/10.1524/ract.2010.1763>.

Primus, P.A., Kumke, M.U., 2012. Flash photolysis study of complexes between salicylic acid and lanthanide ions in water. *J. Phys. Chem. A* 116, 1176-1182,

<http://dx.doi.org/10.1021/jp2043575>.

Rabung, T., Geckeis, H., Kim, J.I., Beck, H.P., 1998a. The influence of anionic ligands on the sorption behaviour of Eu(III) on natural hematite. *Radiochim. Acta* 82, 243-248,

<http://dx.doi.org/10.1524/ract.2000.88.9-11.711>.

Rabung, T., Geckeis, H., Kim, J.I., Beck, H.P., 1998b. Sorption of Eu(III) on a natural hematite: application of a surface complexation model. *J. Colloid Interface Sci.* 208, 153-161,

<http://dx.doi.org/10.1006/jcis.1998.5788>.

Rabung, T., Stumpf, T., Geckeis, H., Klenze, R., Kim, J.I., 2000. Sorption of Am(III) and Eu(III) onto gamma-alumina: experiment and modelling. *Radiochim. Acta* 88, 711-716,

<http://dx.doi.org/10.1524/ract.2000.88.9-11.711>.

Reiller, P., Moulin, V., Casanova, F., Dautel, C., 2002. Retention behaviour of humic substances onto mineral surfaces and consequences upon thorium (IV) mobility: case of iron oxides. *Appl. Geochem.* 17, 1551-1562, [http://dx.doi.org/10.1016/S0883-2927\(02\)00045-8](http://dx.doi.org/10.1016/S0883-2927(02)00045-8).

Reiller, P.E., 2012. Modelling the metal-organic-surface systems: reasons for relative success, failure, and possible routes for peace of mind. *Mineral. Mag.* 76, 1233-1248,

<http://dx.doi.org/10.1180/minmag.2012.076.7.02>.

Reiller, P.E., Brevet, J., Nebbioso, A., Piccolo, A., 2011. Europium(III) complexed by HPSEC size-fractions of a vertisol humic acid: small differences evidenced by time-resolved luminescence spectroscopy. *Spectrochim. Acta, Part A* 78, 1173-1179,

<http://dx.doi.org/10.1016/j.saa.2010.12.075>.

Reiller, P.E., Buckau, G., 2012. Impacts of humic substances on the geochemical behaviour of radionuclides, in: Poinssot, C., Geckeis, H. (Eds.), *Radionuclide Behaviour in the Natural*

Environment: Science, Implications and Lessons for the Nuclear Industry. Woodhead Publishing, Oxford, UK.

Saito, T., Sao, H., Ishida, K., Aoyagi, N., Kimura, T., Nagasaki, S., Tanaka, S., 2010. Application of parallel factor analysis for time-resolved laser fluorescence spectroscopy: implication for metal speciation study. Environ. Sci. Technol. 44, 5055-5060, <http://dx.doi.org/10.1021/es9036995>.

Schindler, P.W., 1991. A solution chemists view of surface chemistry. Pure Appl. Chem. 63, 1697-1704, <http://dx.doi.org/10.1351/pac199163121697>.

Schindler, P.W., Stumm, W., 1987. The surface chemistry of oxides, hydroxides, and oxide minerals, in: Stumm, W. (Ed.), Aquatic Surface Chemistry. Wiley-Interscience, New York, pp. 83-107.

Shiao, S.Y., Egozy, Y., Meyer, R.E., 1981. Adsorption of Cs(I), Sr(II), Eu(III), Co(II) and Cd(II) by Al₂O₃. J. Inorg. Nucl. Chem. 43, 3309-3315, [http://dx.doi.org/10.1016/0022-1902\(81\)80108-X](http://dx.doi.org/10.1016/0022-1902(81)80108-X).

Smith, R.M., Martell, A.E., Motekaitis, R.J., 1998. Critically Selected Stability Constants of Metal Complexes, NIST Standard Reference Database 46 Version 5.0. National Institute of Standards and Technology, Gaithersburg, MD, USA.

Stumm, W., 1997. Reactivity at the mineral-water interface: dissolution and inhibition. Colloids Surf., A 120, 143-166, [http://dx.doi.org/10.1016/S0927-7757\(96\)03866-6](http://dx.doi.org/10.1016/S0927-7757(96)03866-6).

Stumm, W., Morgan, J.J., 1996. Aquatic Chemistry: Chemical Equilibria and Rates in Natural Waters. John Wiley & Sons, Inc, New York, NY, USA.

Takahashi, Y., Tada, A., Kimura, T., Shimizu, H., 2000. Formation of outer- and inner-sphere complexes of lanthanide elements at montmorillonite-water interface. Chem. Lett., 700-701, <http://dx.doi.org/10.1246/cl.2000.700>.

Tan, X.L., Wang, X.K., Chen, C.L., Sun, A.H., 2007. Effect of soil humic and fulvic acids, pH and ionic strength on Th(IV) sorption to TiO₂ nanoparticles. *Appl. Radiat. Isot.* 65, 375-381, <http://dx.doi.org/10.1016/j.apradiso.2006.10.014>.

Vercouter, T., Amekraz, B., Moulin, C., Giffaut, E., Vitorge, P., 2005. Sulfate complexation of trivalent lanthanides probed by nanoelectrospray mass spectrometry and time-resolved laser-induced luminescence. *Inorg. Chem.* 44, 7570-7581, <http://dx.doi.org/10.1021/ic048509j>.

Wang, Z.M., Van de Burgt, L.J., Choppin, G.R., 1999. Spectroscopic study of lanthanide(III) complexes with carboxylic acids. *Inorg. Chim. Acta* 293, 167-177, [http://dx.doi.org/10.1016/S0020-1693\(99\)00234-0](http://dx.doi.org/10.1016/S0020-1693(99)00234-0).